**People's Democratic Republic of Algeria**
**Ministry Of Higher Education and Scientific Research**
**University HAMMA LAKHDER El-Oued**

**Faculty of Technology**

**Department of Electrical Engineering**

**End of Study Thesis**

**In order to obtain the diploma of**

**MASTER ACADEMIC**

**Domain: Technology**

**Sector: Telecommunication**

**Specialty: Telecommunication Systems**

# Theme

## On-chip broadband laser source using chalcogenide glass planar waveguide

**Prepared by:**
- ❖ Ghezal Farid
- ❖ Mebarki Soufiane
- ❖ Chogga Youcef

**Presented in june 2019 in front of the jury composed of:**

| | | |
|---|---|---|
| M. Mohamed Boulila | MAA | President |
| Dr.KHELIL Abdellatif | MCB | Examiner |
| Dr. Abdelkader Medjouri | MCA | Supervisor |

**Academic year: 2018-2019**

**Laboratory of Exploitation and Valorization of Sahara Energy Resources**

# Acknowledgement

Above all, we thank Allah for helping us to do this work.

Firstly, we would like to express our greatest thanks and gratitude to our supervisor Dr. **MEDJOURI ABDELKADER** who gave us this unique opportunity to do this project and for his guidance and support during the last three years. His help was of a great impact on us during the whole period of studying at university.

Also, we would love to express our warm-hearted thanks to all the Teachers, administration staff and the people who have been there for us and stood by us while working on our thesis.

Finally, we would like endlessly to thank our parents for guiding and encouraging us all the time to keep us on the right path as well as brighten up our future and for continually providing their moral, spiritual, emotional, and financial support, the whole time. My Allah bless them. And, we warmly thank our families **GHEZAL, MEBARKI** and **CHOGGA** who have given us support in many ways since our very first day of school.

# Dedications

*I dedicate this work to the woman who gave me birth, the one who*

*sacrificed everything for me: Her time, her happiness and her health, my*

*mother the core of my spirit, May Allah bless her.*

*To my father, the source of enthusiasm and inspiration in my success, who*

*spent sleepless nights working hard in order to make our life a better one,*

*May Allah bless him.*

*To my grandmother and to all the members of my family: my sisters and*

*brothers who also sacrificed everything for my success.*

*My partners Soufiane and Youcef.*

*To my teacher and friend M. Boukoucha Raouf, and all my friends, my*

*colleagues and to all those who love me and who I respect.*

*FARID*

# Dedications

With every sunrise I feel that I owe a huge debt of gratitude for those who taught me and were the main reason for taking the path of knowledge and wisdom.

I warmheartedly dedicate this work to all who encouraged me and supported me and helped me

To my mother who gave birth to me and taught me and lightened my way to climb the ladder of success through every single grade at school.

And to my father the source of my strength and my only idol who inspired me and made me the man I am now.

To my brothers and particularly the youngest who is my source of happiness and joy.

To my partners Farid and Youcef.

Last but not least, to my grandparents, all the members of my family as well as all of my friends and colleagues with my best wishes for a brighter future.

SOUFIANE

# Dedications

*I dedicate this humble work to the purest and dearest person I have ever known, who has always been there for me and supported me, my mother.*

*To the one has brought the best out of me and made me strong enough to face this life and all the hardships, my father.*

*To all my brothers and sisters, uncles and aunts, cousins and distant relatives who helped to pave the way for my success not only in my personal life but also in my academic career.*

*To all my friends and particularly Farid and Soufiane, colleagues and the ones who have ever been by my side encouraging and supporting my steps.*

*To my soulmate who has lit my life and made it warm and colorful, my dear fiancé.*

*YOUCEF*

# Abstract

The work presented in this manuscript concerns the study and modeling of the linear and non-linear properties of optical waveguide (ridge waveguide), and this for create a Broadband laser source on an optical chip using a chalcogenide glass waveguide $As_2S_5$. The linear and nonlinear optical properties have been calculated and optimized by using a fully vectorial finite-difference in the frequency-domain (FDFD) method. The results of simulations show that with a good optimization of the waveguide structure, to exhibit an all normal dispersion (ANDi) profile over the entire computational domain and this by properly adjusting its high and width, we've got a broad and perfectly coherent ultra-flat SC spectrum extending from 700 to 5300 nm, and this is also by exploiting the nonlinear effects that appear in waveguide during the propagation of ultra-short pulses (femtosecond). The physical model and the contribution of different nonlinear effects are presented in numerical modeling, on the other hand, is based on the solution of the generalized nonlinear Schrödinger equation (GNLSE).

**Keywords :**

Optical waveguide, Chromatic dispersion, Supercontinuum generation, Nonlinear optics.

# الـملـخـص

يتعلق العمل المقدم في هذه الاطروحة بدراسة ونمذجة الخصائص الخطية وغير الخطية لمـوجـه الموجة الضوئية ( مـوجـه موجة ريدج)، وهذا لإنشاء مصدر ليزر واسع النطاق على رقاقة بصرية باستخدام  زجاج $As_2S_5$. تم حساب  الخصائص البصرية الخطية وغير الخطية وتحسينها باستخدام طريقة (FDFD). تظهر نتائج عمليات المحاكاة أنه مع التحسين الجيد لهيكل موجه الموجه بما يضمن تبدد طيفي سالب من أجل كل أطوال الأمواج  (ANDi) وهذا عن طريق ضبط ارتفاعه وعرضه بشكل صحيح ، أصبح لدينا نطاق طيفـي SCفائق ومتسق تمامًا و مسطح يمتد من 700 إلى 5300 نانومتر ، وهذا أيضًا عن طريق استغلال التأثيرات غير الخطية التي تظهر في  موجه الموجي أثناء انتشار نبضات قصيرة للغاية (فيمتوثانية). يتم تقديم النموذج المادي ومساهمة التأثيرات غير الخطية المختلفة في النمذجة العددية ،   وذلك بلعتماده على حل معادلة شرودنجر غير الخطية العامة(GNLSE) .


**الكلمات المفتاحية:**

موجه موجي بصري، تبدد طيفي،طيف واسع مستمر ، بصريات لاخطية.

# SUMMARY

## Table of contents

**Chapter III : Simulations results and discussion**

# LISTS OF FIGURES

## *Chapter I*

# *Chapter II*

# *Chapter III*

# LIST OF TABLES

# LIST OF ACRONYMS

**ANDi** all normal dispersion

**As** Arsenic

**As$_2$S$_5$** arsenic pentasulfide

**CAGR** The compound annual growth rate

**ChG** chalcogenide

**FDFD** finite-difference in the frequency-domain

**FWHM** Full width at half maximum

**FWM** Four-Wave Mixing

**Ge** Germanium

**GNLSE** generalised nonlinear Schrödinger equation

**GVD** dispersion of the group velocity

**IR** infrared

**LOC** lab-on-a-chip

**MIR** mid-infrared

**MgF$_2$** magnesium fluoride

**NIR** near-infrared

**O** oxygen

**OWB** Optical Wave Breaking

**PIC** Photonic Integrated Circuit

**S** sulphur

**SOI** silicon-on-insulator

**Sb** Antimony

**SC** Supercontinuum

**SCG** Supercontinuum generation

**Se** selenium

**Si** silicon

**SPM** Self- Phase Modulation

**SRS** Stimulated Raman scattering

**SS** Self-Steepening

**SSFM** Split Step Fourier Method

**Te** Tellurium

**WB** Wave Breaking

**WDM** wavelength-division multiplexed

**XPM** Cross-Phase Modulation

**ZDW** zero-dispersion wavelength

# GENERAL INTRODUCTION

Supercontinuum (SC) generation refers to the considerable spectral broadening through the interaction of intense and short optical pulses with nonlinear materials such as solids, liquids and gases [1]. Since its discovery for the first time in the beginning of the 1970s [2], SC has attracted massive attentions due to its wide applications to metrology, pulse compression, optical communications, coherence tomography, spectroscopy and tunable multi-wavelength laser sources [3].SC arises from a series of nonlinear processes depending on the waveguide chromatic dispersion regime where the femtoseconde pulses are injected, When optical pulses propagate through a highly nonlinear waveguide, their temporal as well as spectral evolution are affected not only by a multitude of nonlinear effects but also by the dispersive properties of the waveguide. All nonlinear processes are capable of generating new frequencies within the pulse spectrum. SC generation relies on the interplay of various nonlinear effects such as Self-Phase Modulation (SPM), Cross-Phase Modulation (XPM), Soliton dynamics, Raman scattering, and Four-Wave Mixing (FWM), and it requires an optical waveguide with suitably designed group velocity dispersion (GVD), including a zero-dispersion wavelength (ZDW) close to the central wavelength of the pump sources. In the anomalous regime (D > 0), SC generation is dominated by soliton-related propagation dynamics [4]. The generated spectra are broad, mainly due to the creation of new pulses resulting from the fundamental Soliton Fission (SF) process. However, these spectra are partially coherent due to their sensitivity to the noise-related pump pulse intensity fluctuations [5]. In the normal regime (D < 0), Self-Phase Modulation (SPM) and Optical Wave Breaking (OWB) are responsible for the spectral broadening. The generated spectra are relatively narrower than in the anomalous dispersion regime, but highly coherent and smooth [6].

Recently, planar waveguides have gained much attention for on-chip SC sources due to their low cost, reduced size and high nonlinear parameter, and have shown also huge potential as SC light sources in the mid-infrared (MIR) region and considerable effort has been channeled into making the processes that lead to the broadening of an injected pulse more efficient, the physics behind the process of SC in optical waveguides has been studied since the results of Ranka et al. and several

tries have been made to explain generated broad bandwidth [7–9]. These waveguide based SC sources are of growing importance for photonic integrated circuits [10], and we are on the cusp of revolutionary changes in communication and microsystems technology through the marriage of photonics and electronics on a single platform. By marrying large-scale photonic integration with large-scale electronic integration, wholly new types of systems-on-chip will emerge over the next few years.

In recent years chalcogenide glasses have appeared as promising nonlinear materials in the mid-infrared region extending from 1 to 14 μm. Chalcogenide glasses contain one or more of the chalcogen elements from group 16 of the periodic table (S, Se, Te but excepting Oxygen) covalently bounded with glass forming materials such as As, Ge and Ga, Si [11,12]. Thanks to their suitable optical properties, they have been widely used to design waveguide based mid-infrared SC sources [11]. Compared to silica, ChG exhibits high optical Kerr nonlinearities, high refractive index and wide transparency window covering near-infrared and mid-infrared [13]. and the combustion rate at Chalcogenide (ChG) glasses is high and it is a good advantage even in increasing optical intensity.

The work described in this thesis was motivated by the need to explore theoretically the design and optimization of optical planar waveguides (ridge waveguide consisting of arsenic pentasulfide ($As_2S_5$) ChG glass strip deposited on magnesium fluoride ($MgF_2$) substrate and air acting as an upper cladding) for SC generation in the MIR regime by utilizing the dispersive and nonlinear properties of the waveguide. The propagation characteristics of the fundamental guided mode such as chromatic dispersion, effective mode area and nonlinearity are calculated by using a finite-difference in the frequency-domain (FDFD) method. The waveguide structure is optimized to exhibit an all normal dispersion (ANDi) profile over the entire computational domain by properly adjusting its high and width. Furthermore, we demonstrate spectral broadening of an intense femtoseconde pulse pumped at 2.5 μm, By solving the generalized nonlinear Schrödinger equation, we demonstrate supercontinuum generation extending from the near infrared to the mid infrared region. Indeed, a broad and perfectly coherent ultra-flat supercontinuum spectrum spanning the region from 700 to 5300 nm is successfully generated by using a 25 kW peak power and 50 fs, input pulse pumped at 2.5 μm, in a waveguide of 5 mm length.

The thesis has been structured as follows:

Chapter 1 presents theoretical overview about the main elements related to the generation of SC on chip that is needed to understand the work presented in this thesis. For an understanding in general, the photonic integrated Circuits (PICs) and its applications as well as types of optical waveguides and overview for supercontinuum generation SCG and its types, applications and chalcogenide material and its features.

Chapter 2 chapter shows the main theory needed to understand results presented in this thesis. Section 1 starts with a few linear effects that occur during pulse propagation inside the optical waveguides. Section 2 reviews the various nonlinear effects responsible for SC generation in the waveguide output. Section 3 introduces the brief overview of generalized nonlinear Schrödinger equation (GNLSE) for modelling pulse propagation in optical waveguides.

Chapter 3 presents that we numerically investigate mid-infrared SC generation in a ridge waveguide. The propagation characteristics of the fundamental guided mode such as chromatic dispersion, effective mode area and nonlinearity are calculated by using a finite-difference in the frequency-domain (FDFD) method. As presents that the waveguide structure is optimized to exhibit an all normal dispersion (ANDi) by properly adjusting its high and width. By solving the generalized nonlinear Schrödinger equation, we demonstrate supercontinuum generation extending from the near infrared to the mid infrared region.

# Chapter I

# State of the art of

# Integrated Photonics

# Introduction

We are on the cusp of revolutionary changes in communication and microsystems technology through the marriage of photonics and electronics on a single platform. By marrying large-scale photonic integration with large-scale electronic integration, wholly new types of systems-on-chip will emerge over the next few years.

Electronic-photonic circuits will play a ubiquitous role globally, influencing such areas as high-speed communications for mobile devices (smartphones, tablets), optical communications within computers and within data centers, sensor systems, and medical applications. In particular, we can expect the earliest impacts to emerge in telecommunications, data centers and high-performance computing, with the technology eventually migrating into higher-volume, shorter-reach consumer applications [14].

## I.1 Definition ofPhotonic Integrated Circuit (PIC)

A photonic integrated circuit (PIC) or integrated optical circuit is a device that integrates multiple (at least two) photonic functions and it is device similar to electronic integrated circuits but use light rather than electrons for information signaling and transfer. While electronic integrated circuits are usually constructedas arrays of transistors, PICs employ a range of components (e.g., waveguides) to focus, split, isolate, polarize, couple, modulate, and, ultimately, detect light. Technical advancements in materials fabrication-realized especially over the past two decades-have enabled embedding these numerous functions in a single small-footprint PIC device [14]. PICs are increasingly applied in telecommunications and sensing platforms and significant research and development (R&D) investments continueto advance a rapidly expanding market (estimated CAGR (The compound annual growth rate) of 31% from 2016 to 2023) [15, 16].
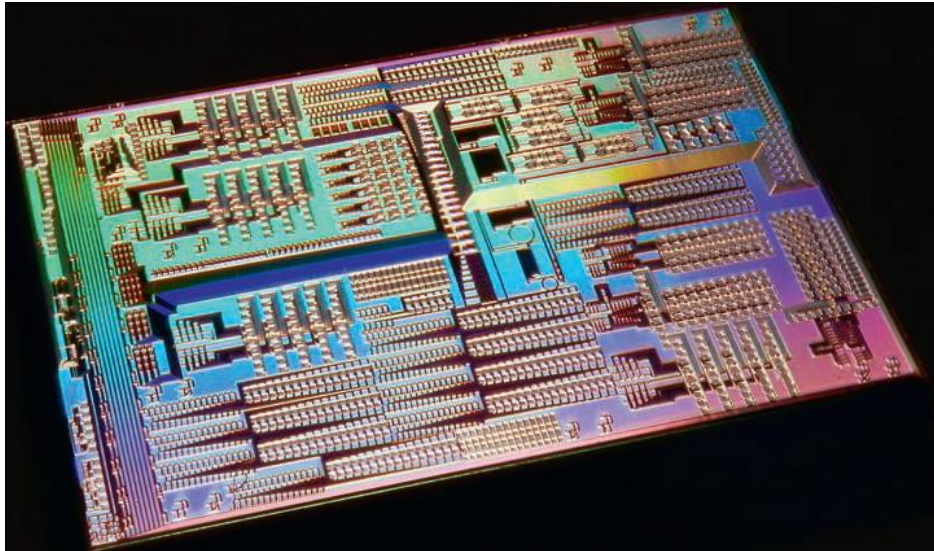
**Fig I.1:** Photograph of SOI photonic chip fabricated at IME A*STAR [17].

Moreover, existing silicon foundries that produce highly controlled wafers (Fig I.2) for microelectronics already exist. The microfabrication infrastructuretodo silicon photonics already exists, in the microelectronics industry. Milestone advancements in this domain have occurred. Several companies aremanufacturing silicon photonic chips, e.g., Luxtera's chips are already used in some high-performance computer clusters [15]. As -Intel© announced the first fully integrated wavelength multiplexed silicon-based photonics chip in 2015,a disruptive advancement to present day information technology architectures [18].
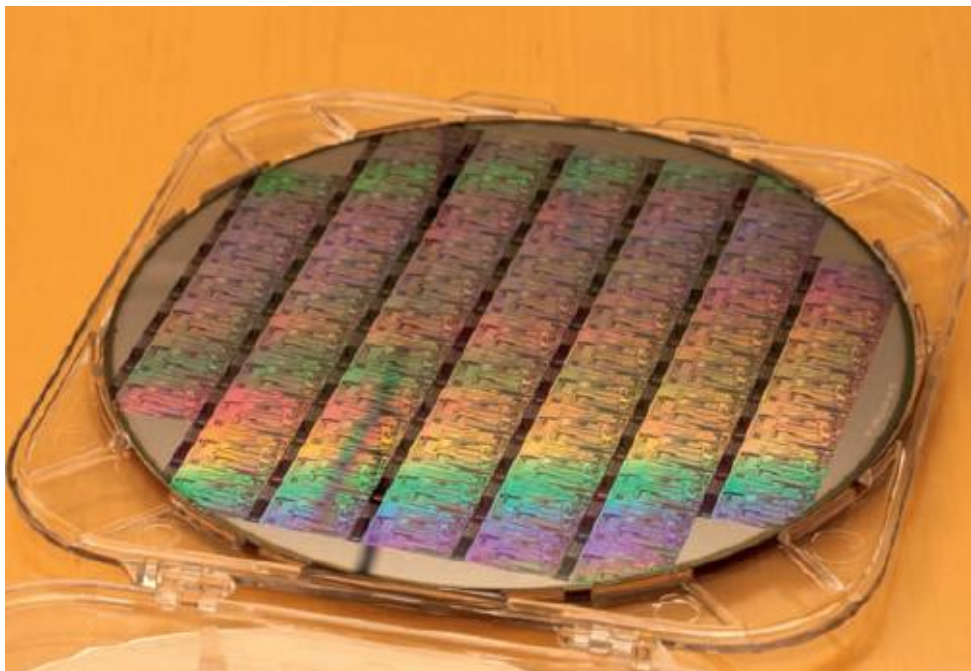


**Fig I.2:** Photograph of  SOI wafer with various photonic components and circuits [19].

Silicon-based Photonic Integrated Circuit development is also driven by the telecommunications industry due to its suitability for transmitting light in the near-infrared (NIR) region of the electromagnetic spectrum. Nevertheless, silicon is not appropriate for all applications and PICs that operate in the mid-infrared (MIR) and other ranges may require different waveguide materials.There are some materials compatible with many applications and their ranges broader than silicon and their refractive index higher than Silicon such as chalcogenides.We are going to focus more about chalcogenide in waveguide in this thesis. Another key challenge with silicon is the realization of truly monolithic and portable lab-on-a-chip (LOC) systems, which include integrated optical sources and detectors on-chip [17,20].

As shown in Fig I.3 there are many components in silicon photonics platform and we are going to study and focus on the waveguide part in this thesis.
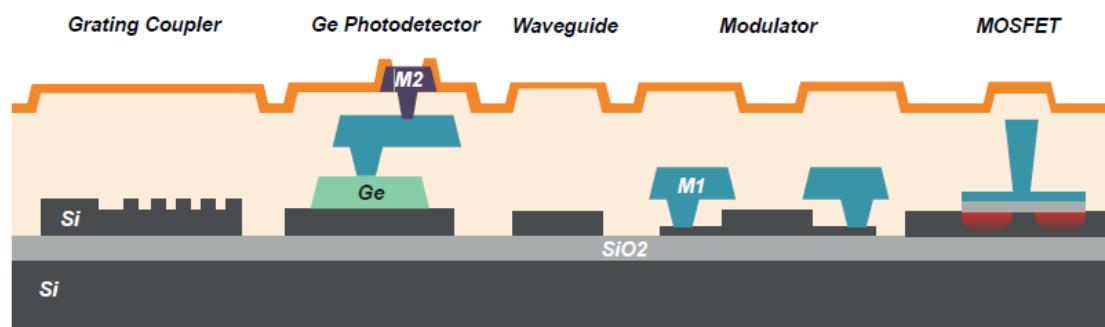


**Fig I.3:** Typical process stack representing a silicon photonics platform with grating couplers, germanium photodetectors, waveguides, modulators and MOSFETs, on asilicon-on-insulator wafer [17,19].

## I.1.1 Comparison to electronic integration

Electronic-photonic circuits will play a ubiquitous role globally, impacting such areas as high-speed communications for mobile devices (smartphones, tablets), optical communications within computers and within data centers, sensorsystems, and medical applications. Table 1 shows the different between Electronic integrated circuits and photonic integrated circuits [21].

| Table I.1\| the different between Electronic integrated circuits and photonic integrated circuits | | |
|---|---|---|
| **Parameters** | Photonic Integrated Circuits | Electronic Integrated Circuits |
| **Mode of function** | Analog | Digital |
| **Materials Used** | InP, GaAs, $LiNbO_2$ ,Si, SOI | Majorty Silicon |
| **Fabrication Technique** | Photolithography | Photolithography |
| **Primary Device (component)** | No particular Device is Dominant | Transistor |
| **Data Transfer Rate** | Data is Transmitted at the speed of light | Data is Transmitted at the speed of Electron Flow |

### I.1.2 Applications

There are a number of applications that are emerging for complex silicon photonic systems, the most common being data communication. This includes high-bandwidth digital communications for short-reach applications, complex modulation schemes and coherent communications for long-reach applications, and so on. Beyond data communications, there are a huge number of new applications being explored in both the commercial and academic worlds for this technology.These include: nano-optomechanics and sensors [22,23], nonlinear optics[24,25], radio frequency integrated optoelectronics [26-28] and coherent communications [29].

### I.2 Optical waveguides

Guided wave optics, realized in both optical fiber and planar technologies, has numerous applications. Optical fibers are the backbone of modern high-speed telecommunication systems. They are also indispensable for the flexible optical power delivery in medical and manufacturing laser applications, high-speed computer interconnects, decreasing the weight, improving immunity to external electromagnetic fields in modern sensor and measurement systems.

Planar optical waveguides, on the other hand, are used for beam formation in edge emitting laser diodes, as sensors in modern sensor and measurement systems, to

provide amplification in optical telecommunication systems, and in high-speed external laser diode modulators.

The optical fibre technology currently allows the fabrication of low loss optical waveguides providing both single mode and multimode wave guiding at a number of wavelengths and for various maximum optical power levels. The fibre optic technology has been advanced and provides many high-quality optical components. The weakness of fibre optic technology lays in the large dimensions of the components and in its limited suitability for low-cost mass production. Planar technology, on the other hand, has the potential to provide the low cost large-scale production of compact optical components, which can meet the demands of the modern telecom systems and other applications [30].

## I.2.1 Optical fiber

Optical fiber is a light transmission medium (transmission channel) in optical systems that allow high-speed data transmission through optical rays.

Optical fiber is usually made of silica, a material that glass. Silica is a compound of silicon (Si) and oxygen (O) whose chemical formula is $SiO_2$[31].
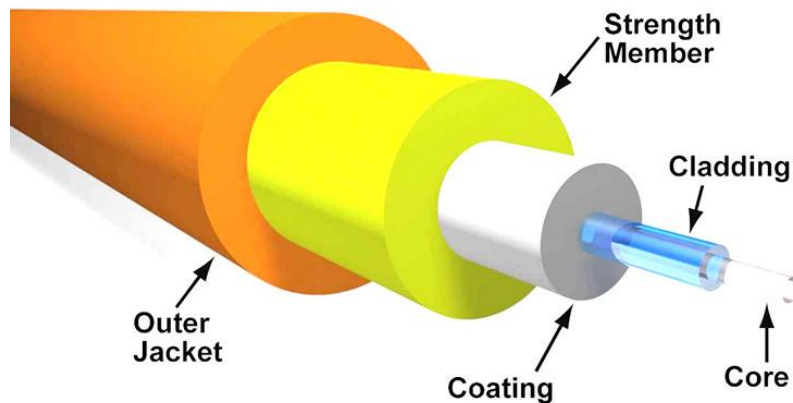


**Fig I.4:** Diagram of an optical fiber [32].

**Core:** the physical component that transports the optical data signal, made up of a continuous strand of glass. the core's diameter is measured in microns.

**Cladding:** the layer that protects the core and causes the necessary reflectionto allow light        to        travel        through        the        fiber-core        segment.

**Coating:** this layer of thicker plastic surrounds the cladding and helps protect the fiber core.

**Strength Member:** the strengthening fibers that help protect the core against damage during installation or from being crushed.

**Outer jacket:** the outermost layer of the fibre cable [33].

## I.2.2 Planar optical waveguides

Recently, planar waveguides have gained much attention for on-chip SC sources due to their low cost, reduced size and high nonlinear parameter, These waveguide based SC sources are of growing importance for photonic integrated circuits [10,34]. The design of a photonic device requires the selection of a particular optical waveguide that meets the design specifications within the parameter space, which is imposed by a selected fabrication technology and device application. The core of the waveguides planar is made of silicon while the cladding is made of silica [7].

These waveguides are extensively used in photonics due to their versatility in terms of application, the large choice of materials they can be made of, and their relatively easy fabrication [8].

There are many types of planar waveguides.We mention some of them

### I.2.2.1Ridge waveguide
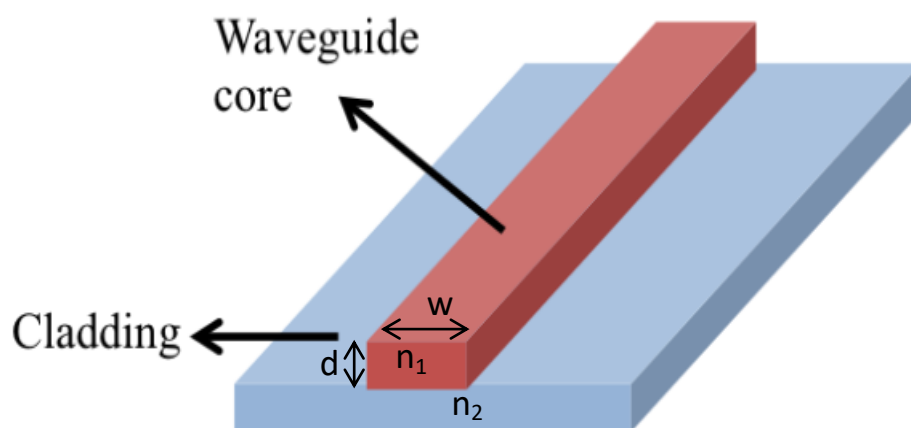


**Fig I.5:**Ridge waveguide[8].

The ridge or strip waveguide, as shown in Figure, consists of a strip of high index material ($n_1$) on a substrate with a lower refractive index ($n_2$). As the surrounding has a lower refractive index ($n_{Air}$) than the strip, light is confined and propagates through the high index medium. The main part of light is confined in the strip which provides both lateral and transverse confinement.

## I.2.2.2 Buried channel waveguide
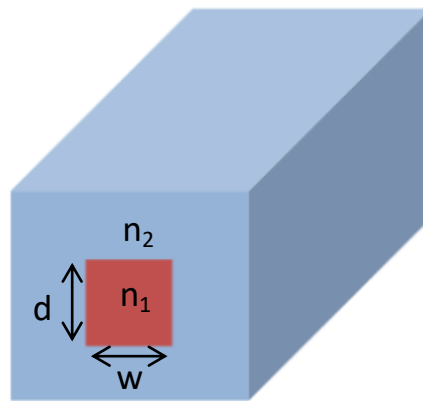


**Fig I.6:**Buried channel waveguide[8].

A buried channel waveguide is formed with a high refractive index waveguide core buried in surrounding medium a low refractive index.

## I.2.2.3 Strip-loaded waveguide
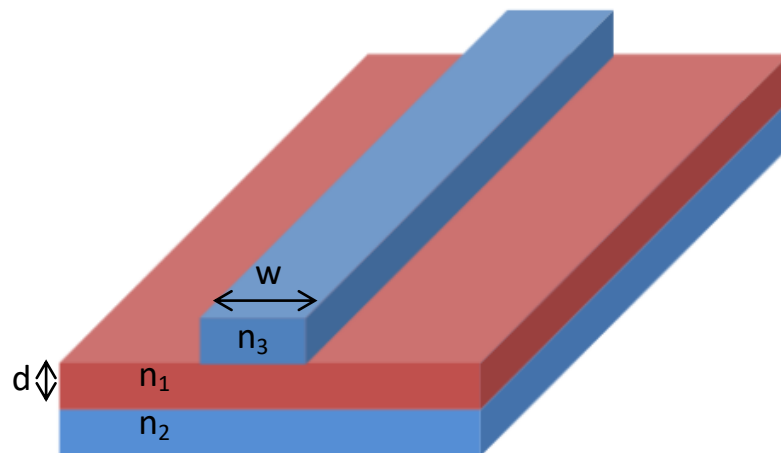


**Fig I.7:**Strip-loaded waveguide[8].

The strip loaded waveguide as shown in Figure consists of a strip(dielectric strip or a metal strip to facilitate optical confinement) of low refractive index material($n_3$) patterned on top of a planar waveguide of higher refractive index material ($n_1$). The loading strip causes a variation in the refractive index which confines light in the horizontal or the y-direction [8].

### I.2.2.4 Rib waveguide
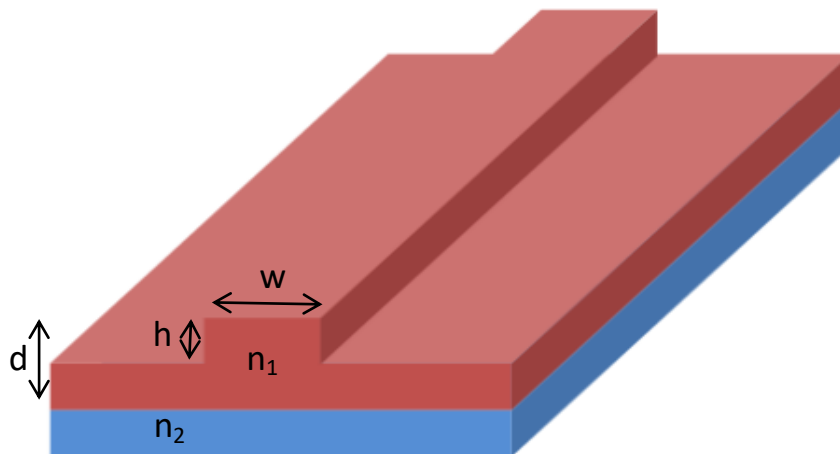


**Fig I.8:**Rib waveguide[8].

A rib waveguide has a structure similar to that of a strip or ridge waveguide, but the strip has the same refractive index as the high refractive index planar layer beneath it and is part of the wave guiding core [9].The slab waveguide confines the propagating light in the vertical or the x-direction.

## I.3 Supercontinuum (SC) generation

The generation of new frequency components with spectral broadening is inherent feature of nonlinear optics and intensively studied since the early1960s. When narrowband incident pulses undergo extreme nonlinear spectral broadening to yield a broadband spectrally continuous output then this process is known as SC generation [35]. SC generation was first observed by Alfano and Shapiro in bulk BK7 glass in 1970 [15, 16], and has since been the subject of numerous investigations in a wide variety of nonlinear optical waveguides. SC arises from a series of nonlinear processes depending on the waveguide chromatic dispersion regime where the femtoseconde pulses are injected. In the anomalous regime (D > 0), SC generation is

dominated by soliton-related propagation dynamics [4]. The generated spectra arebroad, mainly due to the creation of new pulses resulting from the fundamental Soliton Fission (SF) process. However, these spectra are partially coherent due to their sensitivity to the noise-related pump pulse intensity fluctuations [5]. In the normal regime (D < 0), Self Phase Modulation (SPM) and Wave Breaking (WB) are responsible for the spectral broadening. The generated spectra are relatively narrower than in the anomalous dispersion regime, but highly coherent and smooth [6].The figure shows the different between the input pulse and output.
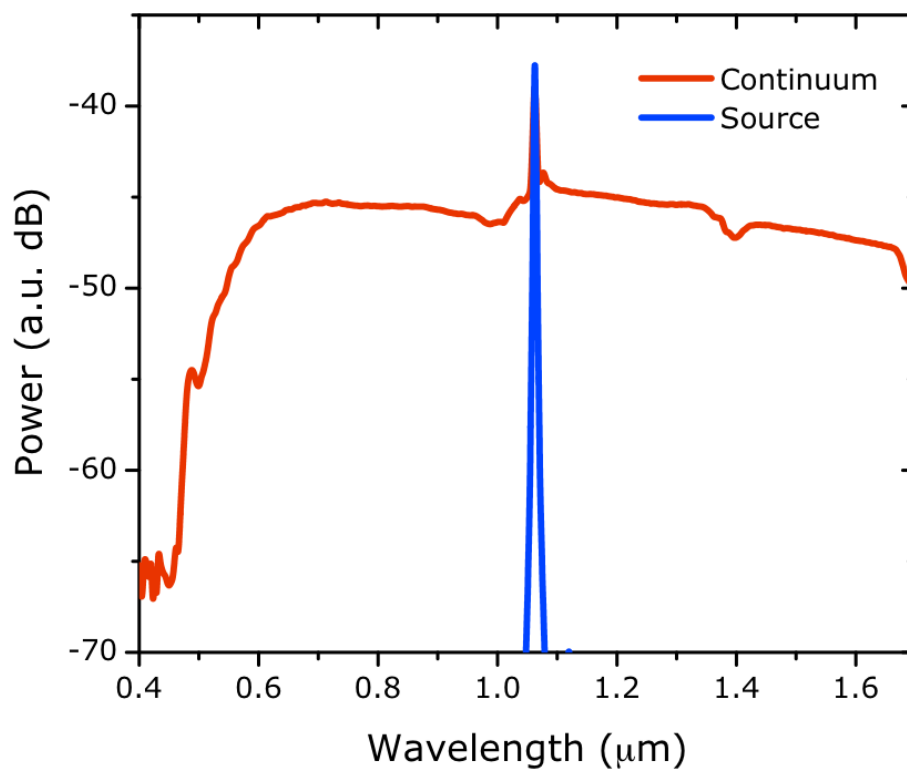


**Fig I.9:** supercontinuum spectrum at initial and the end [36].

Nonlinear optics is an important field of science and engineering because it can generate, transmit, and control the spectrum of laser pulses in solids, liquids, gases, and fibers. One of the most important ultrafast nonlinear optical processes is the supercontinuum generation (the production of intense ultrafast broadband "white light" pulses).

## I.3.1 Types of SC generation

By considering materials state there are:

### I.3.1.1 SC generation in solid, gases and liquids

SC generation was first observed by Alfano and Shapiro 1970 extending the white light spectrum covering the entire visible range from 400 to 700 nm after launching 5 mJ picosecond pulses at 530 nm in bulk BK7 glass [15,16].The bandwidth of SC obtained by the Alfano and Shapiro's experiment was ten-times wider than anything previously reported. Later on Manassah et al. coined this phenomenon assupercontinuum' [37]. In the meantime, the phenomenon of SC generation was referred to as superbroadening [38-40].

By considering properties of guides there are two types: circular guides (optical fibers ) and rectangular guides (planar).

In optical fibers there are SC generation in conventional fibres and SC generation in silica microstructured fibres.

### I.3.1.2 SC generation in conventional fibres

The first SC generation in optical fibres was first observed in 1976 by launching 10 ns pulses from a dyelaser into a 20-m-long fibre [41]. The SC spectrum extended over 180 nm when the peak power was 1 kW. The pulses with duration of 25 ps were launched into a 15-m-long fibre supporting four modes at the input wavelength of 532 nm in a 1987 experiment [42]. The output spectrum extended over 50 nm because of the combined effects of SPM, XPM, SRS, and FWM. Similar results were observed when single-mode fibres were used [43]. In a 1987 experiment, a 1-km-long single-mode fibre was used in which 830 fs input pulses with 530 W peak power produced a 200 nm wide spectrum at the output end of the fibre [44]. Similar features were obtained later with longer pulses [45,46].

In planar there is SC generation in chalcogenide nanowire.

### I.3.1.3 SC generation in chalcogenide nanowire

Recently chalcogenide (ChG) planar optical waveguides have emerged as the key devices to construct scalable, low cost integrated optical circuits such as supercontinuum (SC) laser sources for numerous applications between near-infrared (IR) and mid-infrared (MIR) regimes [47-49]. Among such planar integrated circuits ChG rectangular channel waveguides have shown promising waveguide design for such applications. ChG waveguide enables the generation of MIR SC to above 10 μm due to its wide transmission window as well as the higher nonlinear refractive index ($n_2$), depending on the content of sulphur (S) or selenium (Se) used [50–53].

## I.3.2 Application

- Multi-wavelength Optical Sources

One of the most important applications of SC to the field of telecommunications is the design of multi-wavelength sources for ultra-broadband wavelength-division multiplexed (WDM) systems based on spectral slicing of SC generated by a single laser. As it was mentioned in the previous section, a powerful short optical pulse can be non-linearly broadened into a SC spectrum. This spectrum can then be sliced with an array of filters to create a series of WDM channels [54].

- Pulse Compression and Short Pulse Generation.
- Supercontinuum in optical coherence tomography.

## I.4 Chalcogenide glasses

Recently attention has focused on chalcogenide (ChG) glasses because these glasses exhibit high optical nonlinearities (several hundred times that of silica), are transparent in the MIR region, and can be easily drawn into a fiber form [55]. Clearly, ChG fibres can be used to develop a SC source providing wavelengths beyond 5 μm.

ChG glasses contain the chalcogen elements S, Se, Te, covalently bonded with elements such as Ge, As, Sb and form stable glasses over a wide range of compositions [56]. Their optical properties such as refractive index and nonlinearity can be tuned by the appropriate selection of composition. In general, ChG glasses

possess relatively high refractive indices which in turn increases the nonlinear refractive index.

ChG glasses can provide MIR transparency up to 14 μm when telluride-based materials are employed [57]. For waveguide fabrication a high refractive index is advantageous and allows strong confinement of light, a reduction in the effective mode area and thus an increased nonlinear response [58].
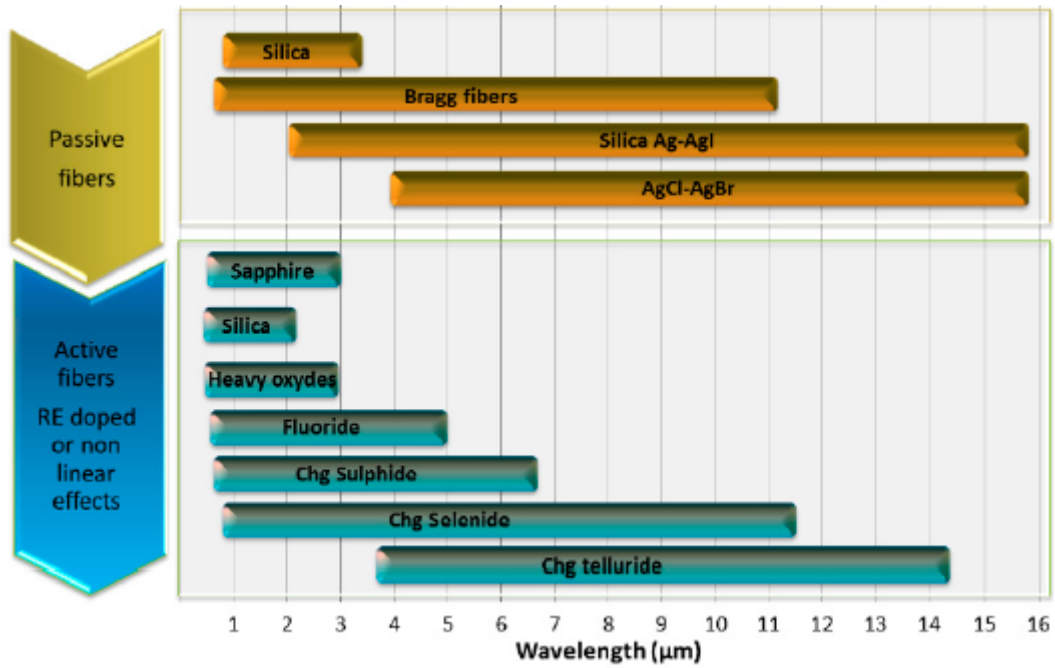


**Fig I.10:** transparency range of some glass types[59].

This table shows refractive index, nonlinear refractive index, transparency and SCG observed with different materials [60].

| Table I.2 \| Linear and nonlinear optical properties of various materials suitable for chip-based nonlinear photonics | | | | |
|---|---|---|---|---|
| **Material** | **refractive index** | **Nonlinear refractive index ($m^2$/w)** | **Transparency ($\mu m$)** | **SCG observed** |
| **SiO$_2$** | 1.45 | $3\times10^{-20}$ | $0.2-4$ | Y |
| **Si** | 3.47 | $5\times10^{-18}$ | $1.2-8$ | Y |
| **AlN** | 2.12 | $2.3\times10^{-19}$ | $0.2-13.6$ | Y |
| **GaN** | 2.31 | $7.8\times10^{-19}$ | $0.36-13.6$ | N |
| **Gap** | 3.05 | $6\times10^{-18}$ | $0.54-10.5$ | N |
| **Diamond** | 2.38 | $8\times10^{-20}$ | $0.22 ->50$ | Y |
| **AlGaAs** | 3.3 | $2.6\times10^{-17}$ | $0.7-17$ | Y |
| **LiNbO$_3$** | 2.21 | $1.8\times10^{-19}$ | $0.35-5$ | Y |
| **As$_2$S$_3$** | 2.43 | $3.8\times10^{-18}$ | $0.6-6.7$ | Y |
| **As$_2$Se$_3$** | 2.81 | $2.4\times10^{-17}$ | $1-11.4$ | Y |
| **As$_2$S$_5$** | 1.85 | $3\times10^{-18}$ | $0.7-5.3$ | Y |
| **Y: yes; N: no. All parameters are values at 1.55 $\mu m$** | | | | |

In this these we are going to work with As$_2$S$_5$glass as mentioned before, that As$_2$S$_5$ exhibits higher optical Kerr nonlinearities, high nonlinear refractive index (n$_2$=3$\times$ 10$^{-18}$) and wide transparency window covering near-infrared and mid-infrared.

## Conclusion

This Chapter gives a theoretical overview of the main elements related to the generation of SC on chip that is needed to understand the work presented in this thesis. For an understanding in general, the photonic integrated Circuits (PICs) aswell as types of optical waveguides and overview for supercontinuum generation SCG and its types, and chalcogenide material and its features.

In this thesis we are going to study SC generation on chip by using rectangular optical waveguide (Ridge waveguide) as well as the material chalcogenide As$_2$S$_5$.

# References

[1] R. Robert. Alfano,"The Supercontinuum Laser Source: The Ultimate White Light", third edition, Springer, (2016),http://dx.doi.org/10.1007/978-1-4939-3326-6.

[2] R.R. Alfano, S.L. Shapiro,"Observation of self-phase modulation and small-scale filaments in crystals and glasses", Phys. Rev. Lett. 24 592–596,(1970),http://dx.doi.org/10.1103/PhysRevLett.24.592.

[3] J.M. Dudley, J.R. Taylor,"Supercontinuum Generation in Optical Fibers", Cambridge University Press,( 2010),http://dx.doi.org/10.1017/CBO9780511750465.

[4] J.M. Dudley, G. Genty, S. Coen,"Supercontinuum generation in photonic crystal fiber", Rev. Mod. Phys. 78 1135–1184,(2006).

[5] A. Hartung, A. M. Heidt, H. Bartelt, "Design of all-normal dispersion microstructured optical fibers for pulse-preserving supercontinuum generation", Opt. Express 19,7742–7749,(2011).

[6] Alexander M. Heidt, Alexander Hartung, Gurthwin W. Bosman, Patrizia Krok, Erich G.Rohwer, Heinrich Schwoerer, Hartmut Bartelt, "Coherent octavespanning near-infrared and visible supercontinuum generation in all-normal dispersion photonic crystal fibers", Opt. Express 19, 3775–3787,(2011).

[7]Shankar Kumar Selvaraja and Purnima Sethi , "Review on Optical Waveguides", Emerging Waveguide Technology, Kok Yeow You, IntechOpen, DOI: 10.5772/intechopen.77150,(2018).

[8] Rajannya sen,"Strip-loaded slot waveguide for highly integrated photonics" Thesis(MA), University of Eastern Finland, (2017).

[9] Younès Messaddeq"Introduction to Dielectric Waveguide" 2nd Edition. Canada: IMI NFG ,(2015).

[10] Dong Yoon Oh, David Sell, Hansuek Lee, Ki Youl Yang, Scott A. Diddams, Kerry J. Vahala, "Supercontinuum generation in on-chip silica waveguide",Opt. Lett. 39 1046–1048,(2014).

[11] A. Zakery, S.R. Elliot, "Optical Nonlinearities in Chalcogenide Glasses and Their Applications", Springer, (2007),http://dx.doi.org/10.1007/978-3-540-71068-4.[12] Stefan Wabnitz, Benjamin J. Eggleton, "All-optical Signal Processing: Data

Communication and Storage Applications", Springer, (2015),http://dx.doi.org/10.1007/978-3-319-14992-9.

[13] N. Granzow, M.A. Schmidt, W. Chang, L. Wang, Q. Coulombier, J. Troles, P. Toupin, I. Hartl, K.F. Lee, M.E. Fermann, L. Wondraczek, P. St. J. Russell,"Mid-infrared supercontinuum generation in $As_2S_3$-silica nano-spike step-index waveguide", Opt. Express 21 (2013) 10969–10977,http://dx.doi.org/10.1364/OE.21.010969.

[14] Jalali B, Fathpour S, "Silicon photonics", J. Lightwave Technol, 24 473 –488, (2006).

[15] "Photonic integrated circuit (IC)—global market outlook (2017-2023)" Stratistics MRC, (2019).

[16] Rohith Chandrasekar, et la, "Photonic integrated circuits for Department of Defense-relevant chemical and biological sensing applications: state-of-the-art and future outlooks", Optical Engineering, 58(2), 020901 (2019).

[17] Lukas Chrostowski, Michael Hochberg, "Silicon Photonics Design", United Kingdom: Cambridge University Press, (2015).

[18] Christy P, "Intel's silicon photonics products could change the world of IT",Google Scholar,(2016).

[19] G. T. Reed and A. P. Knights, "Silicon Photonics", Wileyand sons Online Library, (2008)

[20] Makarona E. et al, "Point-of-need bioanalytics based on planar optical interferometry ",Biotechnol. Adv, 34 209 –233, (2016).

[21] Credence Research  "Photonic Integrated Circuits Market By Integration Technique (Monolithic Integration, Hybrid Integration, Module Integration), By Raw Materials (Indium Phosphide (INP), Gallium Arsenide (GaAS), Silicon, Silicon-On-Insulator (SOI)), By Application (Optical Communication, Sensing, Biophotonics, Optical Signal Processing) - Growth, Share, Opportunities & Competitive Analysis, 2015 – 2022. ",(2016), [Online]. Available from:https://www.credenceresearch.com/report/photonic-integrated-circuits-market[Accessed10/05/19].

# References

[22] M. J. Deen and P. K. Basu, "Silicon Photonics: Fundamentals and Devices" Vol. 43. Wiley,(2012).

[23] Laurent Vivien and Lorenzo Pavesi, "Handbook of Silicon Photonics" CRC Press,(2013).

[24] C. Mead and L. Conway, "Introduction to VLSI Systems" Addison-Wesley series in computer science, Addison-Wesley, isbn: 9780201043587,(1980).

[25]M. Foster, A. Turner, M. Lipson, and A. Gaeta,"Nonlinear optics in photonic nanowires",Optics Express 16.2, pp. 1300–1320,(2008).

[26]J. Capmany and D. Novak,"Microwave photonics combines two words",Nature Photonics 1.6, pp. 319–330, (2007).

[27]Maurizio Burla, Luis Romero Cortés, Ming Li, et al. "Integrated waveguide Bragg gratingsfor microwave photonics signal processing", Optics Express 21.21, pp. 25 120–25 147, (2013).

[28] Tom Baehr-Jones, Ran Ding, Ali Ayazi, et al,"A 25 Gb/s Silicon Photonics Platform", (2012).

[29] Lukas Chrostowski, Nicolas Rouger, Dan Deptuck, and Nicolas A. F. Jaeger, "Silicon Nanophotonics Fabrication: an Innovative Graduate Course", (invited), Doha, Qatar: (invited), doi: 10.1109/ICTEL.2010.5478599,(2010)

[30] Sławomir Sujecki," Photonic Modelling and Design", Boca Raton London New York: Taylor & Francis Group, (2015).

[31] Bedadda Ayman, Guediri Lazhar," Etude et analyse des performances d'un

réseau optique passif large bande bidirectionnel (BPON)", Thesis (MA),University Hamma Lakhder,(2018).

[32] FS,"Fiber Optic Cable vs Twisted Pair Cable vs Coaxial Cable", (2013), [Online] Available from : https://community.fs.com/blog/the-difference-between-fiber-optic-cable-twisted-pair-and-cable.html [Accessed 12/05/19].

[33] FS," A Guide on Fiber Optic Cable", (2013),Available from :https://www.fs.com/a-guide-on-fiber-optic-cable-aid-340.html[Accessed 12/05/19].

[34] Abdelkader Medjouri.et al. "Design and optimization of $As_2S_5$ chalcogenide channel waveguide for coherent mid-infrared supercontinuum Generation", Elsevier, 25 Oct.p. 4,(2017).

[35] N. Bloembergen, "Nonlinear optics: Past, present, and future", IEEE J. Sel, Top. Quantum Electron, 6, pp. 876–880,(2000).

[36] Wikipedia,"Supercontinuum",(2019),[Online] Available from:

https://en.wikipedia.org/wiki/Supercontinuum [Accessed 14/05/19].

[37] J. T. Manassah, P. P. Ho, A. Katz, and R. R. Alfano, "Ultrafast supercontinuum laser source", Photonics Spectra, 18, pp. 53–59, (1984).

[38]W. Werncke, A. Lau, M. Pfeiffer, K. Lenz, H. J. Weigmann, and C. D.Thuy, "An anomalous frequency broadening in water", Opt. Commun,.4, pp.413–415, (1972).

[39] N. Bloembergen, "The influence of electron plasma formation on superbroadening in light filaments", Opt. Commun. 8, pp. 285–288,(1973).

[40]R. L. Fork, C. V. Shank, C. Hirlimann, R. Yen, and W. J. Tomlinson. "Femtosecond white-light continuum pulses", Opt. Lett. 8, pp. 1–3,(1983).

[41] C. Lin and R. H. Stolen, "New nanosecond continuum for excited-stateSpectroscopy", Appl. Phys. Lett., 28, pp. 216–218, (1976).

[42] P. L. Baldeck and R. R. Alfano, "Intensity effects on the stimulatedfour photon spectra generated by picosecond pulses in optical fibers",J. Lightwave Technol. 5, pp. 1712-1715, (1987).

[43] B. Gross and J. T. Manassah, "Supercontinuum in the anomalous groupvelocity dispersion region" J. Opt. Soc. Am. B. 9, pp. 1813-1818, (1992).

[44] P. Beaud, W. Hodel, B. Zysset, and H. P. Weber, "Ultrashort pulse propagation, pulse breakup, and fundamental soliton formation in a single-mode optical fiber", IEEE J. Quantum Electron. 23, pp. 1938-1946 ,1987.

[45]M. N. Islam, G. Sucha, I. Bar-Joseph, M. Wegener, J. P. Gordon, and D. S. Chemla, "Femtosecond distributed soliton spectrum in fibers", J.Opt. Soc. Am. B. 6, pp. 1149-1158, (1989).

[46]I. Ilev, H. Kumagai, K. Toyoda, and I. Koprinkov, "Highly efficient wideband continuum generation in a single-mode optical fiber by powerful broadband laser pumping", Appl. Opt. 35, pp. 2548-2553, (1996).

[47] X. Gai, D. Choi, S. Madden, Z. Yang, R. Wang, and B. Luther-Devies, "Supercontinuum generation in the mid-infrared from a dispersionengineered As2S3 glass rib waveguide", Opt. Lett. 37(18), pp. 3870– 3872,(2012).

[48] Y. Yu, X. Gai, T. Wang, P. Ma, R. Wang, Z. Yang, D. Choi, S. Madden and B. Luther-Davies,"Mid-infrared supercontinuum generation in chalcogenides", Opt. Mater.Exp.3(8),pp.1075–1086,(2013)

# References

[49]Y. Yu, B. Zhang, X. Gai, P. Ma, D. Choi, Z. Yang, R. Wang, S. Debbarma,S. J. Madden, and B. Luther-Davies,"A broadband, quasicontinuous, mid-infrared supercontinuum generated in a chalcogenide glass waveguide", Laser Photonics Rev, pp. 1–7, (2014).

[50]M. R. Karim, B. M. A. Rahman, and G. P. Agrawal,"Mid infrared supercontinuum generation using dispersion-engineered Ge11.5As24Se64.5chalcogenide channel waveguide", Opt. Exp, 23(5) pp. 6903–6914,(2015).

[51] R. J. Weiblen, A. Docherty, J. Hu, and C. R. Menyuk, "Calculation of the expected bandwidth for a mid-infrared supercontinuum source based on As2S3 chalcogenide photonic crystal fibres", Opt. Exp. 18(25), pp. 26666–26674,(2010).

[52] C. Wei, X. Zhu, R. A. Norwood, F. Seng, and N. Peyghambarian,

"Numerical investigation on high power mid-infrared supercontinuum fibre lasers pumped at 3 μm", Opt. Exp. 21(24), pp. 29488–29504,(2013).

[53] I. Kubat, C. R. Petersen, U. V. Mφller, A. B. Seddon, T. M. Benson, L.Brilland, D. Mechin, P. M. Moselund, and O. Bang, "Thulium pumped mid-infrared 0.9-9 μm supercontinuum generation in concatenated fluoride and chalcogenide glass fibres" Opt. Exp.22(4), pp. 3959–3967,(2014).

[54] S.V. Smirnov, J.D. Ania-Castan~on, S. Kobtsev, and S.K. Turitsyn "Supercontinuum in Telecom Applications", Springer Science+Business Media New York,(2016).

[55] X. Gai, T. Han, A. Prasad, S. Madden, D. Y. Choi, R. Wang, D. Bulla, and B. Luther-Davies, "Progress in optical waveguides fabricated from chalcogenide glasses",Opt. Exp.18(25), pp. 26635–26646, (2010).

[56] J. S. Sanghera, L. B. Shaw, L. E. Busse, V. Q. Nguyen, P. C. Pureza, B. C. Cole, B. B. Harbison, I. D. Aggarwal, R. Mossadegh, F. Kung,D. Talley, D. Roselle, and R. Miklos, "Development and infrared applications of chalcogenide glass optical fibers" Fiber and IntegratedOptics, 19, pp. 251–274, (2000).

[57] J. S. Sanghera, L. B. Shaw, L. E. Busse, V. Q. Nguyen, P. C. Pureza, B. C. Cole, B. B. Harbison, I. D. Aggarwal, R. Mossadegh, F. Kung,D. Talley, D. Roselle, and R. Miklos, "Development and infrared applications of chalcogenide glass optical fibers",Fiber and IntegratedOptics.19, pp. 251–274, (2000).

[58] Karim, Mohammad, "Design and optimization of chalcogenide waveguides for supercontinuum generation", Unpublished Doctoral thesis, City University London (2015).

[59] Yiming Wu, Marcello Meneghetti, Johann Troles and Jean-Luc Adam, " Chalcogenide Microstructured Optical Fibers for Mid-Infrared Supercontinuum Generation: Interest, Fabrication, and Applications", Applied sciences,11th sep.pp 2, (2018).

[60] Alexander L. Gaeta 1, Michal Lipson2 and Tobias J. Kippenberg3, "Photonic-chip-based frequency combs", Nat ure Photonics,21th feb, pp 159, (2019).

# Chapter II

# Linear and Nonlinear properties of waveguides

## Introduction

The propagation of an electromagnetic (EM) waves or pulses depends entirely on the medium in which it propagates. In vacuum the pulse can propagate unchanged. When propagating in a medium the EM field interacts with the atoms of the medium. This generally means that the pulse is exposed to loss and dispersion, where the last effect occurs because the different wavelength components of the pulse travel at different velocities due to the wavelength dependence of the refractive index. These effects are termed as the linear response of the medium. If the intensity of a pulse is high enough, the medium also responds in a nonlinear way. The most we can talk about that the refractive index becomes intensity dependent (Kerr effect) and photons can interact with phonons (molecular vibrations) of the medium (Raman effect). In linear optics, signals are only amplified or attenuated but frequencies stay unchanged, while in nonlinear optics, new frequencies can be generated, and a spectrum of a laser pulse can change radically during propagation. As extreme spectral change is indicate to as supercontinuum (SC) generation, a phenomenon first observed in bulk BK7 glass by Alfano and Shapiro in 1970 [1]. These effects are the basis for the many spectral broadening mechanisms, which we will treat further in this chapter.

This chapter shows the main theory needed to understand results presented in this thesis. Section 1 starts with a few linear effects that occur during pulse propagation inside the optical waveguides. Section 2 reviews the various nonlinear effects responsible for SC generation in the waveguide output. Section 3 introduces the brief overview of generalized nonlinear Schrödinger equation (GNLSE) for modelling pulse propagation in optical waveguides.

## II.1 Linear properties of waveguides

### II.1.1 Losses

Loss/attenuation is an important waveguide parameter which provides a measure of power loss during propagation of optical signals inside the waveguide, given by:

$$\alpha\left[dB/m\right] = -\frac{10}{L}\log_{10}\left(\frac{P_T}{P_0}\right) \qquad \text{(II.1)}$$

where $P_0$ is the power launched at the input of a waveguide of length L and $P_T$ is the transmitted power [2]. These processes can be classified into two categories: those that are related to the core material (Chalcogenide) and its quality of manufacture (absorption, diffusion)and others are two more attenuation mechanisms are occurred such as confinement losses and bending losses [3].

## II.1.1.1 Losses by absorption

Absorption of signal is a serious loss mechanism in an optical fiber. This type of loss results in a conversion of photon energy into another form of energy (vibration for example) due to the presence of imperfections in the atomic structure of the fiber material, due to some basic intrinsic material properties and due to some extrinsic material properties. But the contribution from imperfections is relatively small in fiber optic absorption losses. intrinsic absorption is caused by basic fiber material properties. If a material is free from impurities and imperfections, then entire absorption is due to intrinsic absorption. Silica fibers very low intrinsic material absorption. Here, the vibration of silicon-oxygen bonds causes absorption. The interaction between these bonds and the electromagnetic field of the optical signal is responsible for intrinsic absorption. Presence of impurities in the fiber material leads to extrinsic absorption. This is caused by the electronic transition of metal impurity ions from one energy level to another. Another reason for extrinsic absorption is the presence of hydroxyl ions in the fiber[4].

## II.1.1.2 Losses by diffusion

Diffusion losses arise from microscopic variations in the density of the material, fluctuations in composition and inhomogeneity, or defects induced during the manufacturing process of the fiber. In the presence of a scattering center,a propagating wave undergoes diffusion in all directions (Fig.II.1).
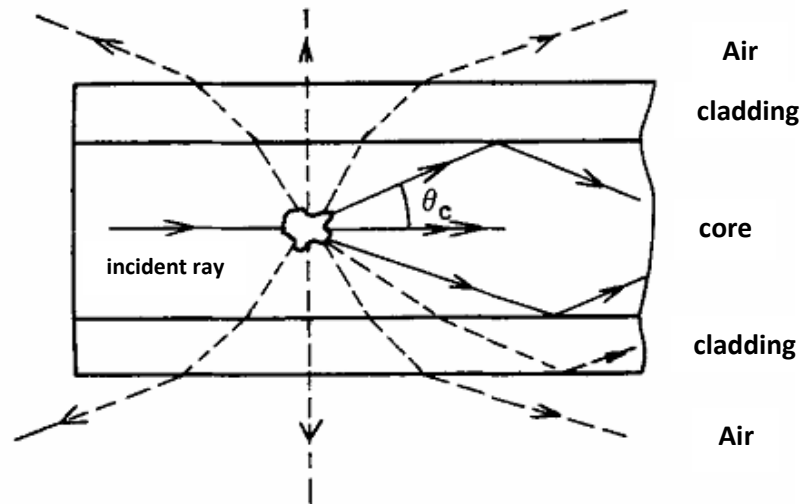
**Fig.II.1:** Diffusion in the core of an optical fiber [3].

Part of the scattered rays emerge from the core of the fiber and disperse in the cladding, thus causing a loss of power of the transmitted light energy, thus a signal attenuation which is a function of λ, and which decreases rapidly when λ increases. There are two types of scattering: linear diffusion (elastic), for which diffused photons keep the same frequency, and nonlinear diffusion (inelastic), for which diffused photons have their frequency modified. There are two linear diffusion subtypes, depending on the size of the scattering center: the Rayleigh scattering that occurs when the dimensions are far smaller than the wavelength and the Mie scattering that manifests itself when the dimensions are the same order of the wavelength.

### II.1.1.3 Confinement losses

The confinement loss is determined by the waveguide, the diameter to pitch ratio in a particular design of microstructured fibre determines how much light leaks from the core into the cladding. The lower the ratio, the more leakage is expected into the cladding. By careful design, the confinement loss can be made as low as required [5,6].

These losses are calculated according to the imaginary part of the effective index of the mode according to the following formula [7]:

$$\alpha \, (dB/km) = \frac{2\pi}{\lambda} \frac{20}{\ln(10)} Im(n_{eff}) \qquad (II.2)$$

## II.1.1.4 Bending losses

Bend loss is caused by bending of the fibre. This is because internal light paths exceeding the critical angle for total internal reflection which mainly depends onwavelength. Theoretically, when the fibre is bent, light propagates outside the bend faster than the inner radius. This is not possible practically and the light is radiated away [7-10].

Two types of bending occur in micro-structured fibres: macro bending and micro bending.

### II.1.1.4.1 Macro bending

is a large scale bending that is visible in which the bend is imposed on optical fibre. The bend region strain affects the refractive index and acceptance angle of the light ray.
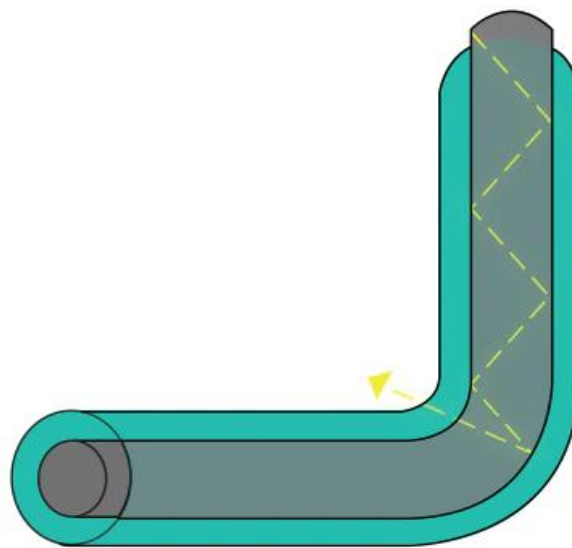


**Fig II.2:**Macro bending [11].

### II.1.1.4.2 Micro bending

is a small scale bend that is not visible which occurs due to the pressure on the fibre that can be as a result of temperature, tensile stress of force and so forth. It affects refractive index and refracts out the ray of light and thus loss occurs [7].
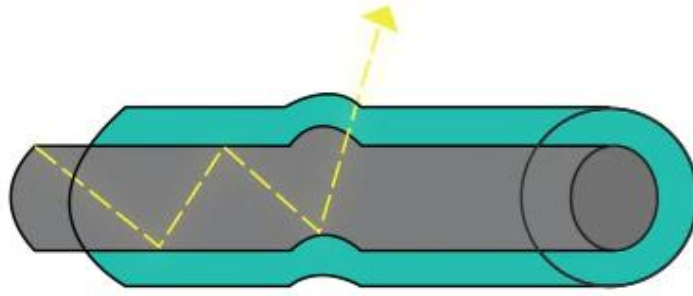
**Fig II.3:**Micro bending[11].

## II.1.2 Dispersion

An optical waveguide is dispersive when the effective index of its fundamental mode is a function of the wavelength. Thus a pulse propagating in an optical fiber will undergo a more or less significant time spread depending on its central wavelength and its time width[3].

By changing the waveguide dispersion (altering the fibre design) and balancing it against the materiel dispersion (fixed), the dispersion characteristics of the fibre can be engineered to required values[7].

$$D_c = D_m + D_g \tag{II.3}$$

### II.1.2.1 Chromatic dispersion

Since the pulse has a nonzero spectral width around the frequency $f_0$, we can use Taylor's development around the $w_0$ pulse to express the propagation constant $\beta$ at the pulsation $w$[3]:

$$\beta(w) = n_{eff}\frac{w}{c} = \beta_0 + \beta_1(w-w_0) + \frac{1}{2}\beta_2(w-w_0)^2 + \frac{1}{6}\beta_3(w-w_0)^3 + ... \tag{II.4}$$

And

$$\beta_m = \left(\frac{d^m\beta}{dw_m}\right)_{w=w_0} \quad m = 0, 1, 2, 3\ldots \text{ [2]} \tag{II.5}$$

The term $\beta_1$ is inversely proportional to the group velocity $v_g$ of the wave[3]

$$\beta_1 = \frac{1}{v_g} = \frac{1}{c}\left( n + w\frac{dn}{dw} \right) \tag{II.6}$$

The value of $\beta_2$ reflects the variation of the group velocity vg between two different wavelengths, the dispersion of the group velocity GVD is expressed by the variable $\beta_2$ according to:

$$\beta_2 = \frac{1}{c}\left( 2\frac{dn}{dw} + w\frac{d^2n}{dw^2} \right) \tag{II.7}$$

In the domain of optical fibers, the term is used "chromatic dispersion", referred to as $D_c$, expressed in( ps / (nm.km) ), given by[10]:

$$D_c = -\frac{2\pi c}{\lambda}\beta_2 \tag{II.8}$$

Nonlinear effects in optical waveguides can manifest qualitatively different behaviors depending on the sign of the GVD parameter. If parameter D is negative ($\beta_2 > 0$), this is the normal dispersion regime where the red components of the pulse travel faster than the blue components, i.e. positive chirp. Similarly, if D is positive ($\beta_2 < 0$), i.e. anomalous dispersion regime, where the red components of the pulse travel slower than the blue components, i.e. negative chirp. When $D = 0$, which corresponds to the zero-dispersion wavelength (ZDW), all frequency components of the pulse travel at the same speed (to lowest order) and the pulse maintains its original shape[3].

## II.1.2.2 Materiel Dispersion

The refractive index of chalcogenide is wavelength dependent. Different wavelength has different refractive index. This is called material dispersion [7]. This variation is often expressed by the Sellmeier formula given by [2]:

$$n(\lambda) = \sqrt{1 + \sum_{j=1}^{m}\frac{A_j\lambda^2}{\lambda^2 - \lambda_j^2}} \tag{II.9}$$

With:

| Table II.1 | Sellmeier coefficients of As$_2$S$_5$ and MgF$_2$ glasses | | |
| --- | --- | --- | --- |
| **As$_2$S$_5$** | | **MgF$_2$** | |
| **A$_j$ $\lambda_j$** | | **A$_j$ $\lambda_j$** | |
| 2.1361 | 0.3089 | 0.48755708 | 0.0433840 |
| 0.0693 | 15 | 0.39875031 | 0.09461442 |
| 1.7637 | 4.66 x 10$^{-4}$ | 2.3120353 | 23.793604 |

The dispersion of material is given by[3]:

$$D_m = -\frac{\lambda}{c}\frac{d^2 n_m}{d\lambda^2}$$

(II.10)

The dispersion due to the material and described until now is not the only contribution to the chromatic dispersion of an optical fiber. Indeed, we must not forget to add the dispersion introduced by the guide itself[12].

### II.1.2.3 Waveguide Dispersion

This is due to the fact that light is in fact not strictly confined to the core. The electric and magnetic fields constituting the light impulse actually extend (a little) outside the core, therefore in the cladding. The electromagnetic field "overflows" in the cladding all the more as the wavelength is large. The refraction index seen by the wave is therefore an average between the refractive index of the core and that of the cladding. The smaller wavelengths will therefore tend to propagate more slowlythan the longer wavelengths, resulting in an enlargement of the light pulse[13].

As for guide dispersion, its expression is given by[3]:

$$D_g = -\frac{\lambda}{c}\frac{d^2 n_{eff}}{d\lambda^2}$$

(II.11)

## II.2 Nonlinear properties of waveguides

### II.2.1 Wave Equation

Understanding nonlinear phenomena in optical fibers requires studying the theory of electromagnetic wave propagation in nonlinear dispersive media. Like any electromagnetic phenomenon, the propagation of optical fields is governed by the Maxwell equations that lead to the wave equation, given by: [14]

$$\nabla \times \nabla \times \vec{E}\left(\vec{r},t\right) = -\frac{1}{c^2}\frac{\partial^2 \vec{E}\left(\vec{r},t\right)}{\partial t^2} - \mu_0 \frac{\partial^2 \vec{P}\left(\vec{r},t\right)}{\partial t^2} \qquad \text{(II.12)}$$

The constant $\mu_0$ then corresponds to the magnetic permeability of the vacuum and c is the speed of light in a vacuum (299,792,458 m / s).

Under the influence of an electric field E, it is possible to deform the electronic cloud locally: this is the phenomenon of electronic polarization. This phenomenon is likely to create many microscopic electrostatic dipoles. The field seen locally by the material then results from the field applied to the material and the induced polarization field. When the applied electric field is weak, the induced polarization is proportional to this field, the material has a so-called linear response, it is called linear polarization $P_L$. When the applied field reaches values of the order of magnitude of the intra-atomic fields, the polarization of the material then becomes a non-linear function ($P_{NL}$) of the electric field E and is expressed according to the following relations [3]:

$$P = P_L + P_{NL} \qquad \text{(II.13)}$$

$$P_L = \varepsilon_0 \chi^{(1)} E \qquad \text{(II.14)}$$

$$P_{NL} = \varepsilon_0 \left( \chi^{(2)} EE + \chi^{(3)} EEE + ... \right) \qquad \text{(II.15)}$$

For low intensities of the electric field, the development can be truncated at its first term; the polarization then depends linearly on the E field. The real and imaginary part of the linear susceptibility $\chi^{(1)}$ corresponds to the refractive index of the material n and to the linear absorption coefficient α. For intense field strength, the

influence of higher order terms ceases to be negligible. The susceptibility of order 2: $\chi^{(2)}$ is responsible for non-linear effects such as second harmonic generation and sum frequency generation. However, it is null for media with inversion symmetry at the molecular level. Therefore, for glass which is a symmetrical molecule, $\chi^{(2)}$ is zero. As a result, glass is mainly the seat of non-linear effects originating from the 3-fold susceptibility: $\chi^{(3)}$, which is responsible for nonlinear inelastic phenomena such as stimulated Raman or elastic phenomena such as the optical Kerr effect responsible for many effects such as self-phase modulation (SPM), cross-phase modulation (XPM), four-wave mixing (FWM). [14]

## II.2.2 The Kerr effect

The propagation of an intense optical field in an optical fiber causes an instantaneous change in the refractive index of the medium. This phenomenon is called optical Kerr effect. The refractive index is then dependent on the intensity of the optical field and is decomposed in two:

$$n\left(w,t\right) = n_{L}\left(w\right) + n_{2}I(t) \qquad\qquad \text{(II.16)}$$

Where $n_L$ corresponds to the linear index, I(t) the intensity of the field and $n_2$ the nonlinear index of the medium. The refractive index then consists of a linear component related to the dielectric susceptibility of the first order and a nonlinear component related to the dielectric susceptibility of the third order. When the intensityof the electric field is low, the non-linear contribution to the refractive index can be neglected. If not, it must be taken into account.

For a fiber in ChG($As_2S_5$) $n_2$ is equal to $3\times10^{-18}$ $m^2$ / W[15], this value depends in particular on the presence of possible dopants and the measurement technique. This nonlinear index is directly related to the susceptibility of order three by the relation[10]:

$$n_{2} = \frac{3}{8n_{L}}\text{Re}\left[\chi^{(3)}\right] \qquad\qquad \text{(II.17)}$$

For an optical fiber, the Kerr effect isexpressed by its factor $\gamma$ given by:

$$\gamma = \frac{n_2 w_0}{c A_{eff}} \qquad (II.18)$$

where $w_0$ is the pulsation, c is the celerity of the light and $A_{eff}$ is the effective area relative to the guided mode.

### II.2.2.1 Self-Phase Modulation

Under a strong field intensity, the variation of the refractive index causes a self-induced phase shift. This effect is called self-phase modulation (SPM).SPM creates new frequencies and can lead to the spectral broadening of optical pulses, which arises due to the time dependence of the nonlinear phase shift i.e. the instantaneous optical frequency changes across the pulse[2].The nonlinear phase shift induced by the self-phase modulation is given by:[3]

$$\Delta\phi_{SPM}(t) = n_2 k_0 L I(t) \qquad (II.19)$$

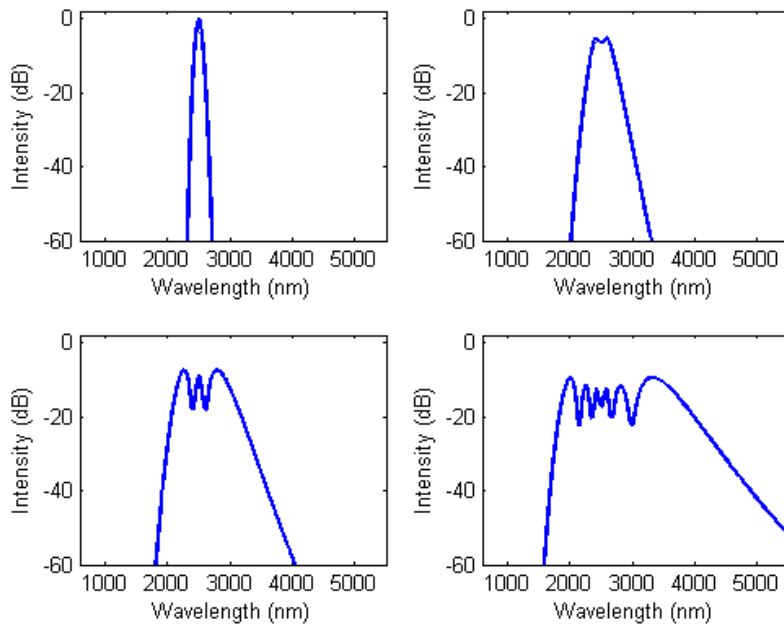give a graphical representation of the self-phase modulation induced by a Gaussian impulse.



**Fig II.4:** Gaussian pulse evolution that having undergone SPM in different regions of the waveguide.

## II.2.2.2 Cross-Phase Modulation

If we consider two optical fields of wavelengths $\lambda_1$ and $\lambda_2$ different, co-propagating in a fiber of length L. Each field is susceptible to generate its own SPM and to undergo an additional nonlinear phase shift induced by the other wave. This phenomenon is called Cross Phase Modulation (XPM)[14], and the additional phase shift received by the first wave is written, in the case where the two waves are polarized along the same axis[12, 16]:

$$\Delta\phi_{XPM}\left(t\right) = 2n_2 k_0 I_2 L = 2\gamma P_2 L \qquad \text{(II.20)}$$

with $I_2$ ($P_2$) the intensity (power) of the second wave. The XPM phase shift is generally responsible for an asymmetrical spectral broadening of the pulses with respect to their initial frequencies. This asymmetry is due to the difference in the group velocities between the two spectral components[14].

## II.2.2.3 Four Wave Mixing

Four wave mixing (FWM) describes a nonlinear process in which four optical waves interact with each other as the consequence of the third order susceptibility $\chi^{(3)}$. The origin of FWM is in the nonlinear response of bound electrons of a material to an electromagnetic field [2]. FWM process involve nonlinear interaction between four optical waves oscillating at frequencies $\omega_1$, $\omega_2$, $\omega_3$, and $\omega_4$. Generally, there are two types of FWM process. First corresponds to the case in which three photons transfer their energy to a single photon at the frequency $\omega_4 = \omega_1 + \omega_2 + \omega_3$. Second corresponds to the case in which two photons at frequency $\omega 1$ and $\omega 2$ are destroyed, while two photons at frequencies $\omega_3$ and $\omega_4$ are created simultaneously, so that

$\omega_3 + \omega_4 = \omega_1 + \omega_2$.

The efficiency of FWM depends strongly on the phase matching of the frequency components and consequently relies on dispersion properties of the optical waveguide[2].

## II.2.3 Self-Steepening

Self-steepening is a higher order nonlinear effect which results from the intensity dependence of the group velocity. It causes an asymmetry in the SPM broadened spectra of ultrashort pulses as the pulse moves at a lower speed than the wings of the pulse [17]. Therefore, as the pulse propagates inside the waveguide, the peak shifts towards the trailing edge and the trailing edge becomes steeper with increasing distance. Self-steepening of the pulse creates an optical shock and is only important for short pulses [2].

## II.2.4 Raman Scattering

The effects of scattering, Raman and Brillouin, were the first nonlinear effects studied in optical fibers [18]. Unlike the Kerr effect, the Raman and Brillouin effects are due to an exchange of energy between the optical field and the dielectric medium, which is called inelastic effects. Nevertheless, the Brillouin effect does not contribute to the generation of the supercontinuum in the femtosecond regime because the threshold of its appearance is higher compared to that of Raman. In addition, the Brillouin effect is manifested only with long-lasting pulses ($> 1$ ns) [19]. Here we describe the phenomenon of stimulated Raman scattering [20].

During the propagation of an intense optical field in a nonlinear medium, a photon of the pump wave at the frequency $\omega_p$ is diffused into a photon of frequency $\omega_s$, the energy difference being absorbed by the scattering center. The excitation of the medium is reflected, most often, by a modification of the vibrational or rotational level of the molecules. The process gives rise to a lower frequency photon (Stokes wave) or a higher frequency photon (anti-Stokes wave). However, in the presence of the pump wave $\omega_p$ and the signal wave $\omega_s$, an amplification process of the wave $\omega_s$ at the expense of the wave $\omega_p$ can take place. This is called stimulated diffusion [21]. This amplification process can be very efficient ($> 10\%$ of the value of the pump wave). Fig. 5 shows the process of Raman scattering.
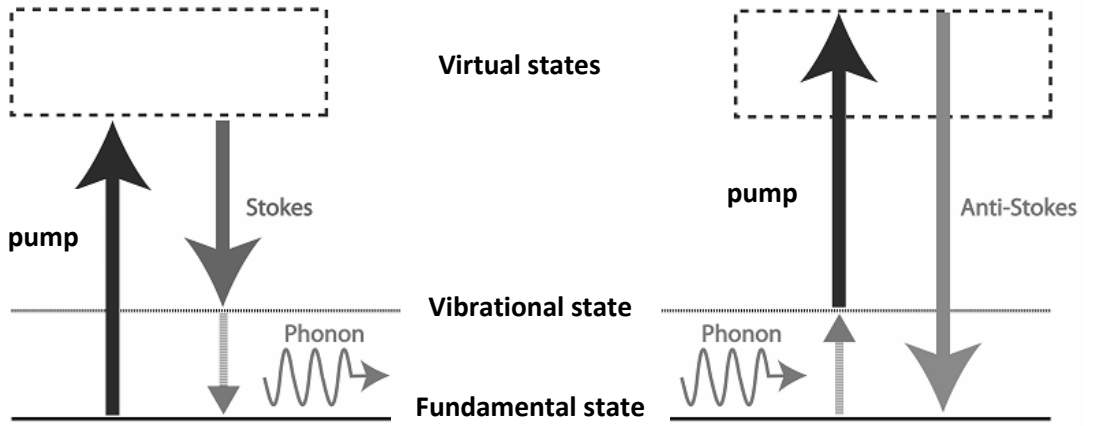
**Fig II.5:** Raman scattering process [22].

## II.3 Generalized Nonlinear Schrödinger Equation (GNLSE)

The change in pulse envelope A as the pulse propagates along the fibre axis z is described by the generalized nonlinear Schrödinger equation (GNLSE) [17]

$$\frac{\partial A}{\partial z} + \frac{\alpha}{2}A - D'A = i\gamma(1 + i\tau_{shock}\frac{\partial}{\partial T})\left( A(z,t)\int_{-\infty}^{\infty} R(T') \times |A(z,T-T')|^2 \, dT' \right)$$

(II.21)[3-5]

In the Eq (II.21), relating to the total dispersion of the fiber, we thus find

$$\beta_k = \left( \frac{\partial^k \beta}{\partial w^k} \right)_{w=w_0} \tag{II.22}$$

Describing the derivative of order k of the propagation constant with respect to ω [23].

$$D' = \sum_{k \geq 2} \frac{i^{k+1}}{k!} \beta_k \frac{\partial^k A}{\partial T^k} \tag{II.23}$$

αis the linear propagation loss.

The non-linear effects involved during propagation in a fiber can be identified. In this case, the magnitude of these effects is determined by the nonlinear coefficient γ according to: [22].

$$\gamma = \frac{w\,n_2}{c\,A_{eff}} \tag{II.24}$$

The effective area of the propagation mode of the fiber can be calculated according to Eq. (II.25) from the transversal distribution of the mode of guidance in the frequency domain Få (x, y, ω):[22].

$$A_{eff}(w) = \frac{\left( \int\int_{-\infty}^{+\infty} \left| \vec{F}(x, y, w) \right|^2 dxdy \right)^2}{\int\int_{-\infty}^{+\infty} \left| \vec{F}(x, y, w) \right|^4 dxdy} \tag{II.25}$$

The result of this expansion leads to obtaining an optical shock term $\tau_{shock}$ in order to take into account the dispersion of the non-linearity as a function of ω:

$$\tau_{shock} = \frac{1}{\omega_0} \tag{II.26}$$

Finally the material response function includes both the instantaneous electronic response (Kerr type) and the delayed Raman response and has the form [2]:

$$R(t) = (1 - f_R)\delta(t) + f_R h_R(t) \tag{II.27}$$

$$h_R(t) = \frac{\tau_1^2 + \tau_2^2}{\tau_1 \tau_2^2} \exp\left(-\frac{t}{\tau_2}\right)\sin\left(\frac{t}{\tau_1}\right) \tag{II.28}$$

where $f_R = 0.11$, $\tau 1 = 15.2$ fs, and $\tau 2 = 230.5$ fs are taken as for chalcogenide material.[16]

## II.3.1 Types of pulse envelopes

From a general point of view, two main forms of initial pulse envelopes A having a peak power $P_0$ are used. We thus distinguish the impulses of Gaussian type and secant hyperbolic type. [22]

### II.3.1.1 Gaussian pulse

$$A_{Gauss}(z = 0, T) = \sqrt{P_0} \exp\left(\frac{-T^2}{2T_0^2}\right) \tag{II.29}$$

with $T_0$ the half-width (at the point of intensity $P_0 / e$), but in practice we use more easily the total width at half height $T_{FWHM}$ instead of $T_0$. For a Gaussian pulse, the relation is:

$$T_{FWHM} = 2 \left( ln2 \right)^{1/2} T_0 \approx 1.665 \, T_0 \tag{II.30}$$

## II.3.1.2 Hyperbolic secant pulse

$$A_{\text{sech}}(z = 0, T) = \sqrt{P_0} \, \text{sech}\left( \frac{T}{T_0} \right) \tag{II.31}$$

with $T_0$ connected to the total width at half height $T_{FWHM}$ by the relation:

$$T_{FWHM =} 2.ln\left(1 + \sqrt{2}\right) T_0 \approx 1.763 T_0 \tag{II.32}$$

Although the pulses emitted by a large number of lasers correspond to a Gaussian profile, hyperbolic secant pulses are usually considered, particularly in the context of optical solitons and pulses emitted by mode-locked lasers[14].

# Conclusion

This Chapter gives a theoretical overview of the physics related to the generation of SC that is needed to understand the work presented in this thesis.For an understanding of the linear(losses and dispersion) and nonlinear phenomena(the Kerr effect,Self-Steepening and Raman scattering) as well as their effects during propagation of optical signal inside the waveguide it is necessary to introduce the GNLSE that governs the propagation of optical field in the waveguide. Finally, a few of the most relevant nonlinear effects and concepts responsible for propagation dynamics of SC generation have been reviewed.

# References

[1] R. R. Alfano and S. L. Shapiro, "Emission in the region 4000 to 7000 A via four-photon coupling in glass",Phys. Rev. Lett., 24(11), pp. 584–587, (1970).

[2]Karim, Mohammad, "Design and optimization of chalcogenide waveguides for supercontinuum generation", Unpublished Doctoral thesis, City University London, (2015).

[3] Medjouri Abdelkader, "étude des fibres optiques microstructurees et de leurs application aux systèmes optoélectroniques", thesis (PhD), University of Sciences and Technologie Houari Boumediène, (2016).

[4] Ramcha Ndra Kamath, "Optic fibre communication", (2012).

[5] H. Ebendorff-Heidepriem, K. Furusawa, D. R. Richardson, and T. M Monro,

"Fundamentals and applications of silica and non-silica holey fibres", Proc. SPIE, Photonics West, San Jose, (2004).

[6] J. C. Baggett, T. M. Monro, J. R. Hayes, V. Finazzi, and D. J. Richardson, "Improving bending losses in holey fibres", in Proceedings of OFC, Anaheim, (2005).

[7] Colin Yao,"What is Chromatic Dispersion in Optical Fibers", Online Library Fosco. Connect,(2011).

[8] J. P. Goure and I. Verrier, "Optical Fibre Devices", Cornwall, MPG Books

Ltd, (2002).

[9] G. P. Agrawal, "Applications of Nonlinear Fiber Optics", Academic pressNew York, (2008).

[10] F. Poli, A. Cucinotta, and S. Seller, "Photonic crystal fibres propertiesand applications", Dordecht, Springer, (2007).

[11] Cablesys, "Loss in Fiber Optic Performance", Online Library CABLESYS, (2018).

[12] Bertrand Kibler,"Propagation non-linéaire d'impulsions ultracourtes dans les fibres optiques de nouvelle génération", thesis (PhD), University of Franche-Comté, (2007).

[13] Lefievre Rodolphe, "La fibre optique et la technologie WDM", Online Library IGM, (2003).

[14] Rim CHERIF, "Étude des Effets Non-Linéaires dans les Fibres à Cristaux Photoniques", Thesis (PhD) The Higher School of Communications Tunis, (2009).

[15] Abdelkader Medjouri.et al, "Design and optimization of $As_2S_5$ chalcogenide channel waveguide for coherent mid-infrared supercontinuum Generation", Elsevier, 25 Oct.p. 4, (2017).

[16] Stolen R. H and C.H. Lin, "Self-phase modulation in silica fibers", Physical Review A 17, 1448-1453, (1978).

[17] G. P. Agrawal, "Nonlinear Fiber Optics" 5th ed, Academic press, San Diego, California, (2013).

[18] Kuppuswamy Porsezian and Ramanathan Ganapathy, "Odyssey of Light in Nonlinear Optical Fibers: Theory and Applications", Taylor & Francis, (2016).

[19] G. P. Agrawal, "Nonlinear fiber optics", Academic press, Third edition, (2001).

[20] E.P. Ippen and R.H. Stolen, "Stimulated Brillouin scattering in optical fibers", Applied Physics Letters, 21(11), 539-540, (1972).

[21] K. J. Blow and D. Wood, "Theoretical description of transient stimulated Raman scattering in optical fibers", Quantum Electronics, 25(12), 2665 – 2673, (1989).

[22] Benjamin Wetzel, "études expérimentales et numériques des instabilités non-linéaires et des vagues scélérates optiques", Thesis (PhD) University of Franche-Comté, (2012).

# Chapter III

# Simulations resultsand discussion

## Introduction

We numerically investigate mid-infrared SC generation in a ridge waveguide consisting of arsenic pentasulfide ($As_2S_5$) ChG glass strip deposited on magnesium fluoride ($MgF_2$) substrate and air acting as an upper cladding. The propagation characteristics of the fundamental guided mode such as chromatic dispersion, effective mode area and nonlinearity are calculated by using a finite-difference in the frequency-domain (FDFD) method. The waveguide structure is optimized to exhibit an all normal dispersion (ANDi) profile over the entire computational domain by properly adjusting its high and width. Furthermore, we demonstrate spectral broadening of an intense femtoseconde pulse pumped at 2.5 µm. By solving the generalized nonlinear Schrödinger equation, we demonstrate supercontinuum generation extending from the near infrared to the mid infrared region.

## III.1 Structure of the proposed $As_2S_5$ ridge waveguide

The cross sectional view of the proposed ridge waveguide is given by Fig III.1 As mentioned in the previous section, the proposed ridge waveguide consists of $As_2S_5$ strip deposited on $MgF_2$ substrate, and air acting as an upper cladding. The parameters W and H are the core width and high, respectively. The wavelength dependent refractive index of the core and the cladding are given via the Sellmeier equation:

$$n(\lambda) = \sqrt{1 + \sum_{j=1}^{m} \frac{A_j \lambda^2}{\lambda^2 - \lambda_j^2}} \qquad \text{(III.1)}$$

Were the coefficients are given in Table III.1 [1, 2].



**Fig III.1:** Cross sectional view of the proposed $As_2S_5$ ridge waveguide where the width and the high of the channel are W and H, respectively [3].

| Table III.1 Sellmeier coefficients of As$_2$S$_5$ and MgF$_2$ glasses | | | |
|---|---|---|---|
| **As$_2$S$_5$** | | **MgF$_2$** | |
| **A$_j$ $\lambda_j$** | | **A$_j$ $\lambda_j$** | |
| 2.1361 | 0.3089 | 0.48755708 | 0.0433840 |
| 0.0693 | 15 | 0.39875031 | 0.09461442 |
| 1.7637 | 4.66 x 10$^{-4}$ | 2.3120353 | 23.793604 |

The variation of the refractive index with wavelength for both As$_2$S$_5$ and MgF$_2$ is depicted in Fig III.2 The large index contrast between the core and the cladding permits a strong light confinement inside the core whatever its wavelength. The inset Fig III.2 shows the optical field distribution at the excitation wavelength 1 μm and 4 μm respectively[3].
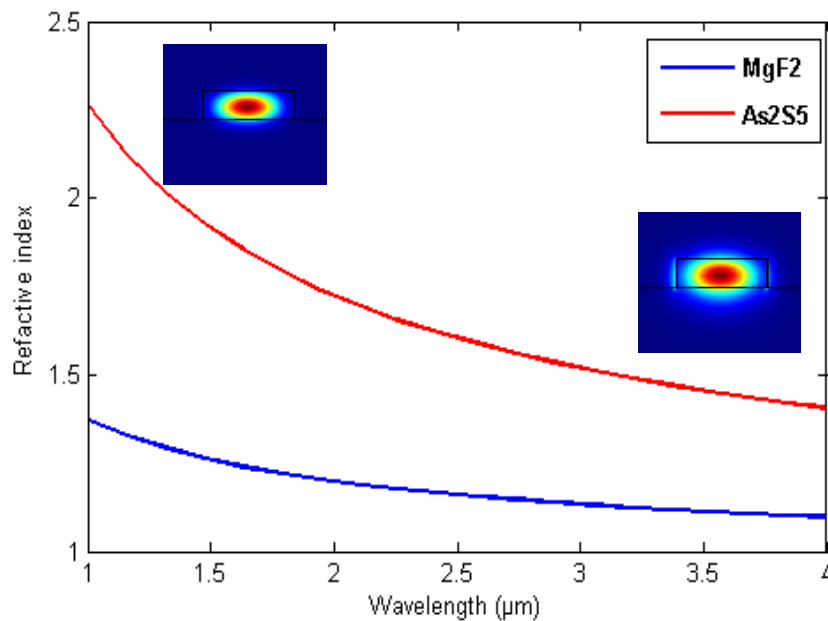


**Fig III.2:** Material refractive index versus wavelength of the As$_2$S$_5$ chalcogenide and MgF$_2$ glass.

## III.2 Structure optimization

As mentioned previously, we aim to optimize the waveguide structure exhibiting negative dispersion so that the generated SC is relatively coherent and

noise insensitive over the entire bandwidth. In order to achieve all normal dispersion ($\beta_2 > 0$) over a wide wavelength range, the structural parameters of the proposed ridge waveguide are suitably adjusted. The impact of both the width (W) and the high (H) is carefully investigated through several numerical simulations. First, we analyzed the effect of W on the dispersion parameter. FigIII.3 shows the evolution of the chromatic dispersion with wavelength for the fundamental TE mode with W = 2 µm and H varying from 0.6 µm to 0.8 µm with step of 0.05 µm. From the figure we observe that dispersion curve increases when H increases too with a peak moving toward long wavelengths. Hence, ANDi (all normal dispersion) regime with a peak close to the zero can be achieved for H laying between 0.6 µm and 0.65 µm. For this respect, we investigated the impact of changing W when H is set to 0.625 µm. FigIII.4 depicts the evolution of dispersion parameter for different values of W ranging from 1.8 µm to 2.4 µm with a step of 0.2 µm. As we can see, the curves shift upward, with an invariant peak, when W decreases. Moreover, the ANDi regime with a peak close to the zero can be obtained for H laying between 2.2 µm and 2.4 µm. Therefore, and from the above results, one can optimize the design of the proposed waveguide in order to achieve the desired ANDi profile over a wide range of wavelengths. For this purpose, we have calculated the chromatic dispersion for the waveguide parameters W = 2.25 m and H = 0.625 m.



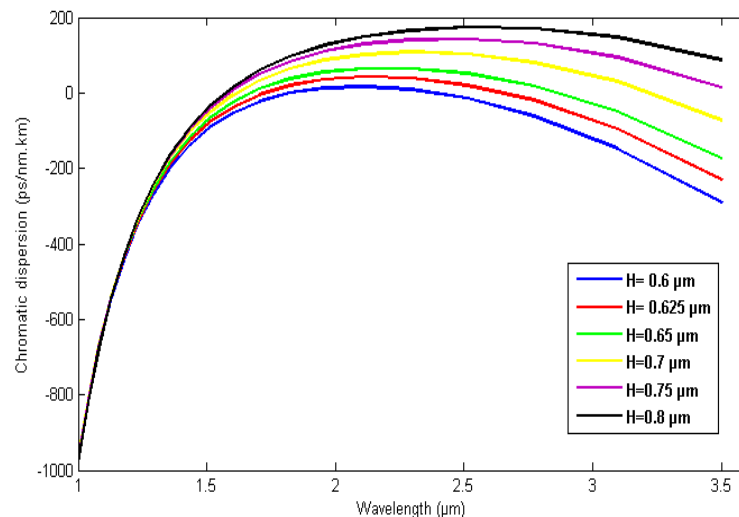**Fig III.3:** Variation of the chromatic dispersion with wavelengths for W=2µm and H changing from 0.6µm to 0.8µm.
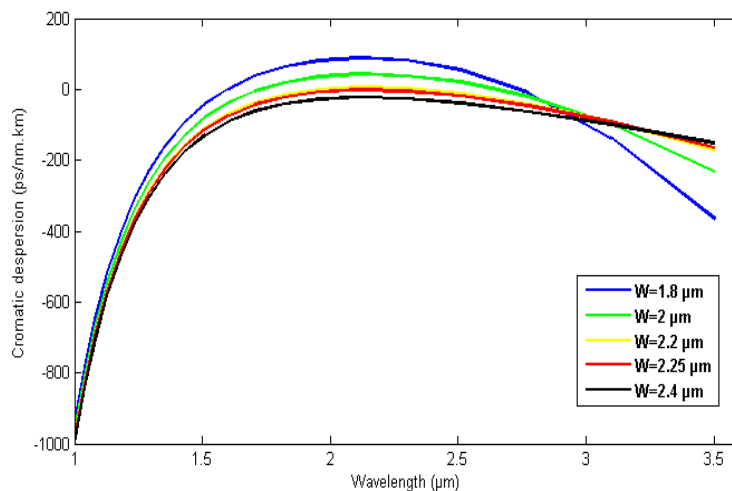
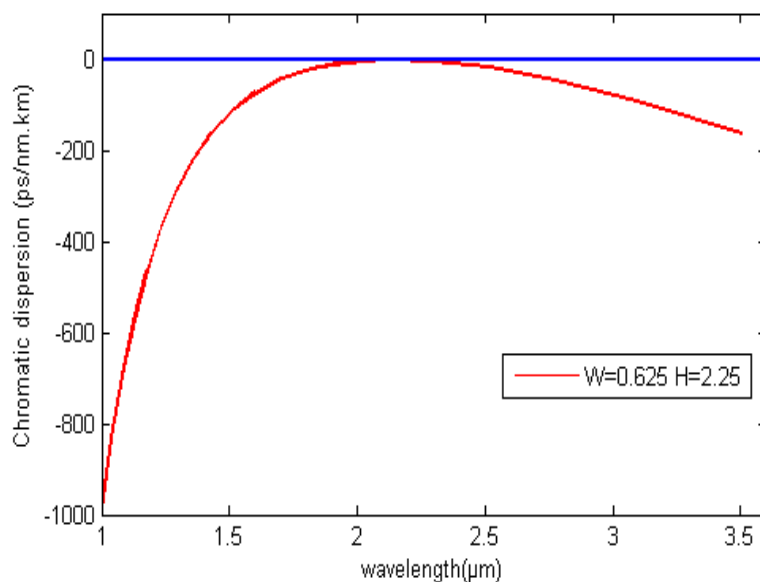**Fig III.4:** Variation of the chromatic dispersion with wavelengths for H=0.625 μm and W changing from 1.8 μm to 2.4 μm.



**Fig III.5:** Variation of the chromatic dispersion with wavelengths for H=0.625 μm and W = 2.25 μm.

As plotted in Fig III.5, the optimized design exhibits a negative dispersion over the whole wavelength range with a zero dispersion around 2µm.

## III.3 SC generation in the optimized design

SC generation was, then, carried out in the proposed chalcogenidewaveguide with the optimized parameters. We consider theinjection of a chirpless Gaussian pulse given by[3]:

$$A(0,t) = \sqrt{P_0} \, e^{\left(\frac{-t^2}{2T_0^2}\right)}$$

(III.8)

where, $P_0$ is the peak power and $T_0$ is the pulse duration related to the pulse Full Width Half Maximum (FWHM) as

$$T_0 = FWHM / 1.665$$

(III.9)

In order to generate broad SC, the pulse is pumped close to the zero dispersionat 2.5 µm. The chromatic dispersion and the nonlinear coefficient at thepump wavelength are −18 ps/nm.km and $0.5 \times 10^4$ W$^{-1}$km$^{-1}$, respectively.



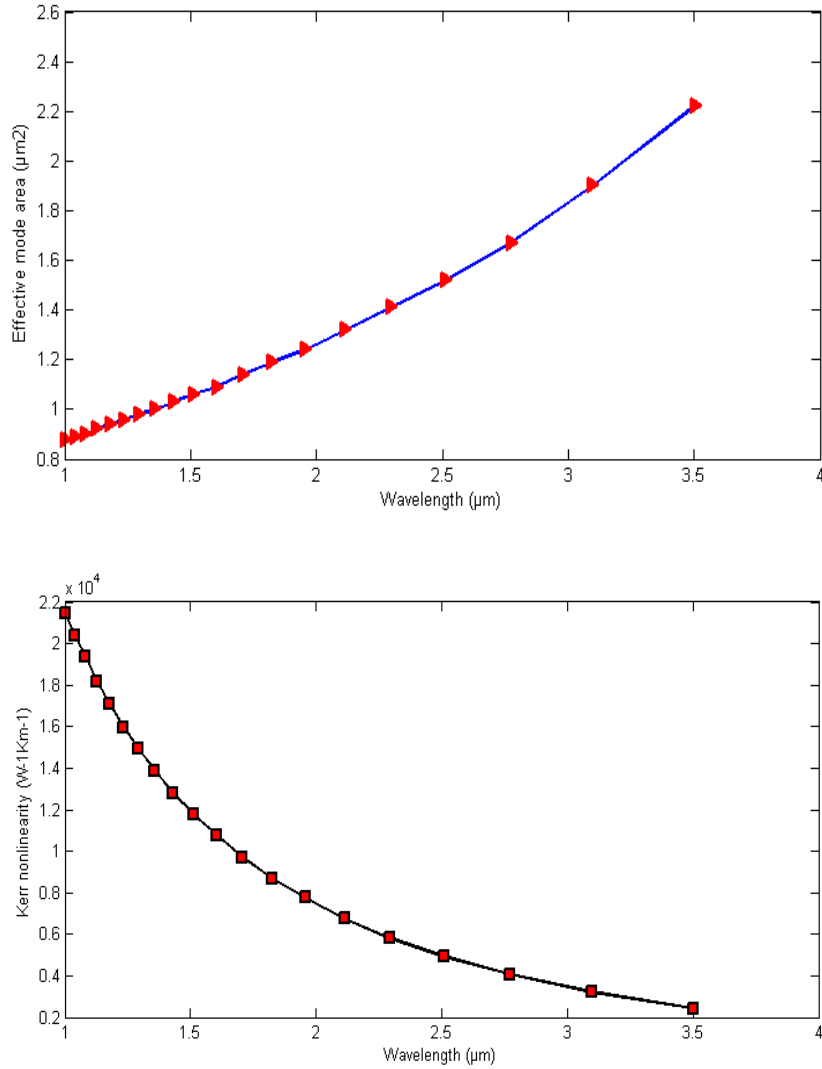**Fig III.6:** Variation of the effective mode area and the corresponding nonlinear coefficient with wavelength for H = 0.625 µm and W = 2.25 µm

We have computed both the effective mode area and the Kerr nonlinear coefficient. Their evolution against wavelength is depicted in Fig III.6 where we, clearly, observe that the waveguide exhibits high nonlinearity up to $2.2 \times 10^4$ w$^{-1}$km$^{-1}$. This is due to, jointly, the small effective mode area and the high nonlinear refractive index.

| Coefficient | Valeur |
|---|---|
| **Table III.2\|** The Taylor series expansion coefficients, up to the 10$^{th}$ order, of the propagation constant have been calculated around the carrier frequency and their values are given in this table | |
| $\beta_2$ | 0.0791 ps$^2$/km |
| $\beta_3$ | - 0.0012 ps$^3$/km |
| $\beta_4$ | $1.5202 \times 10^{-5}$ ps$^4$/km |
| $\beta_5$ | $-1.4895 \times 10^{-7}$ ps$^5$/km |
| $\beta_6$ | $1.4122 \times 10^{-9}$ ps$^6$/km |
| $\beta_7$ | $-1.1137 \times 10^{-11}$ ps$^7$/km |
| $\beta_8$ | $6.4771 \times 10^{-14}$ ps$^8$/km |
| $\beta_9$ | $-2.4170 \times 10^{-16}$ ps$^9$/km |
| $\beta_{10}$ | $4.3176 \times 10^{-19}$ ps$^{10}$/km |

## III.3.1 First Simulation
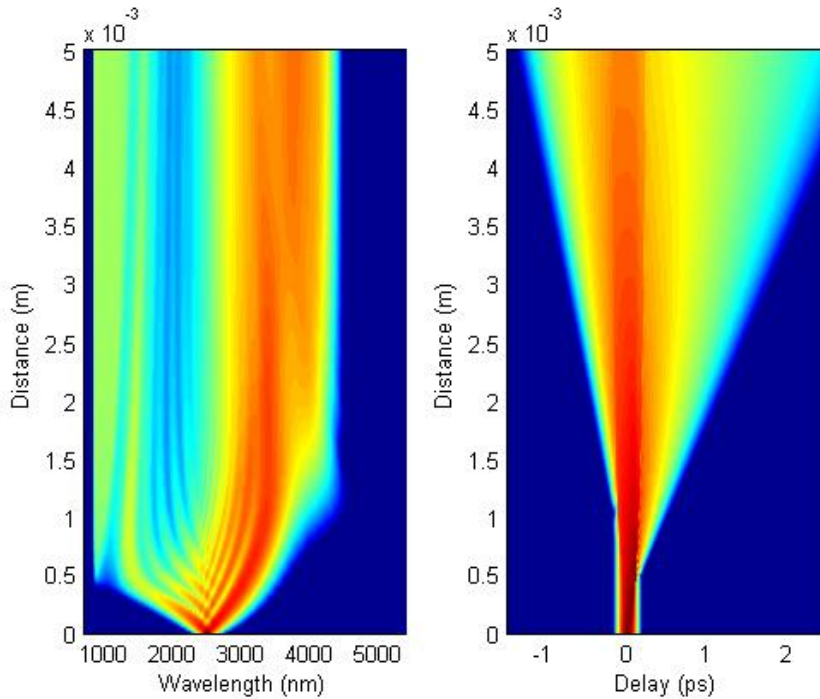


**Fig III.7:** Spectral and temporal evolution over 5 mm waveguide length of a Gaussian pulse with a peak power and FWHM of 10 kW and 100 fs, respectively.

First of all, in the aim to provide a simple physical interpretation of pulse spectral broadening in our proposed design, we have done the first simulation with initial pulse at Peak Power 10 kw and FHWM of 100 fs propagating over 5 mm waveguide length. As we can see Fig III.7 shows the spectral and temporal evolution of the SC generation process over the propagation distance. And it can be noticed that from the pulse spectral evolution, the pulse spectrum begins to broaden due to SPM, SPM create new frequencies so that's why the pulse spectrum begins to broaden automatically. This can be, clearly, observed from the oscillatory structure that appears in the generated spectrum in the first few millimeters [4]. And the Fig III.8 Explains more about the oscillation of SPM that shown in Fig III.7.
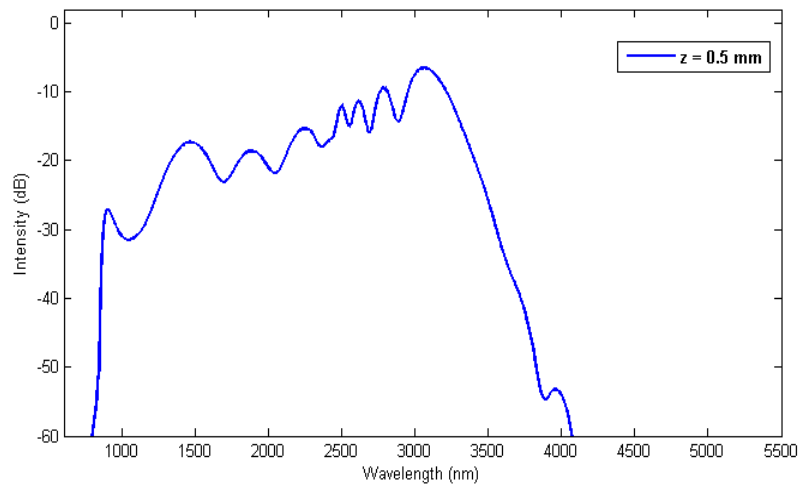


**Fig III.8:** Spectral evolution at 0.5 mm waveguide length.

Then, at a certain point, the pulse is exposed to breaking this is called Optical Wave Breaking (OWB) .

### III.3.1.1 Optical Wave Breaking (OWB)

A new effect appears in femtosecond optical pulse compression, using single-mode fibers, that we describe as Optical Wave Breaking (OWB). In the fiber, frequency-shifted light in the leading and trailing edges of a pulse overtakes unshifted light in the pulse tails [5].

The optical wave breaking appears (OWB) when N > 1, OWB is veryweak and in fact is not observable in case of N < 1. [6]

So for calculate The distance where the OWB is first observed, there are some parameters we have to calculate before , Therefore, the dispersion length $L_D$ given by [3] :

$$\mathbf{L_D} = \frac{\mathbf{T_0^2}}{|\beta_2|} = \mathbf{0.0405\,m}$$

(III.10)

And the nonlinear length $L_{NL}$ given by:

$$\mathbf{L_{NL}} = \frac{1}{(\gamma\,\mathbf{P_0})} = 2\times10^{-5}\,\text{m}$$

(III.11)

the soliton order N can be calculated as following:

$$N = \sqrt{\frac{L_D}{L_{NL}}} = 45$$

(III.12)

Furthermore, the SC spectra start to broaden asymmetrically due to the effect of OWB. The distance where the OWB is first observed is given by [7]:

$$z = \sqrt{\frac{L_D}{4e^{-\frac{3}{2}}N^2 - 1}} = 0.95mm$$

(III.13)

For this simulation, the distance is found to be 0.95 mm. Fig III.9  shows the pulse at the input as well as after 0.95 mm of propagation. Moreover, an overlap of two pulse components with different instantaneous frequencies results in sinusoidal beats between those frequencies [8]. These oscillations indicate the appears of OWB [9]. With further propagation, OWB fully develops by transferring energy from the pulse center wavelengths to the new frequency band around 3900 nm.
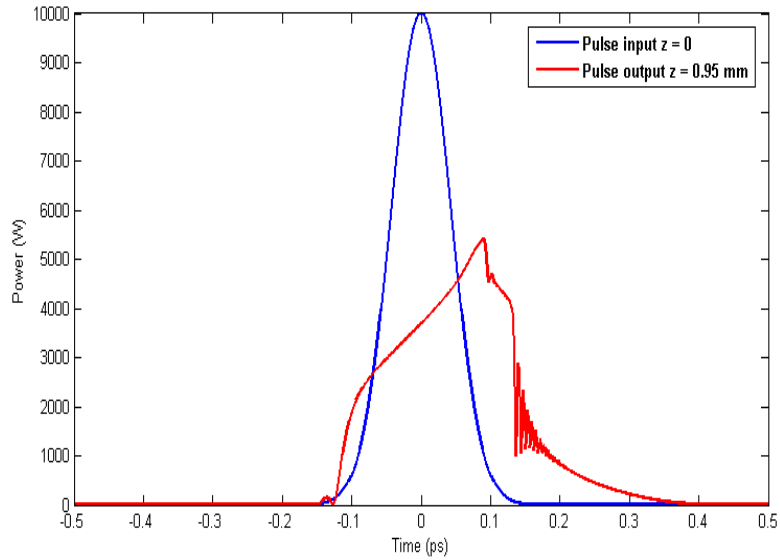
**Fig III.9:** Pulse profiles at the input and after z = 0.95 mm of propagation.
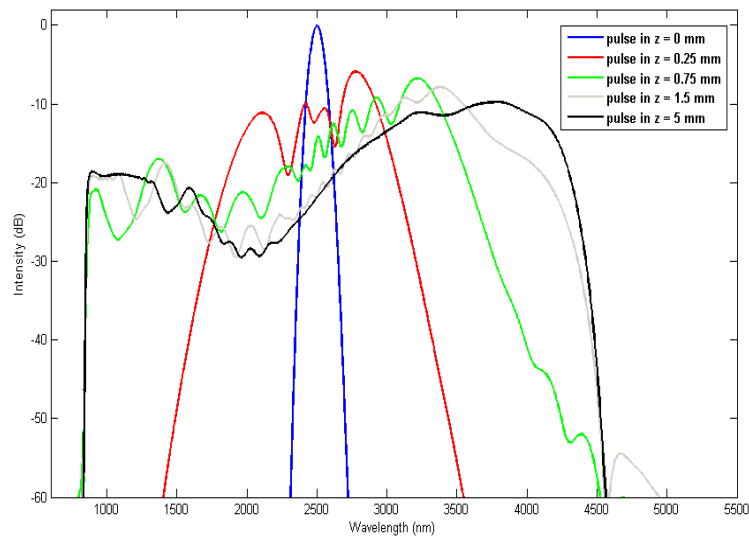
## III.3.1.2 Spectrums at different distances



**Fig III.10 :** Different spectrums of the SC generation process at different distances.

Second of all, in the aim to provide a simple physical interpretation of pulse spectral broadening in our proposed design, we have done first simulation again But by focusing on the shape of the spectrum at different distances with initial pulse at Peak Power 10 kw and pulse duration at FHWM = 100 fs, propagating over 5 mm

waveguide length, as we can see Fig III.10 shows the different spectrums of the SC generation process at different distances. And it can be noticed that when distance increase, the spectrum width increases too, and the pulse form changes too with distance,in in this case the spectrum approximately stay at same form from z = 1.5 mm to z = 5 mm.

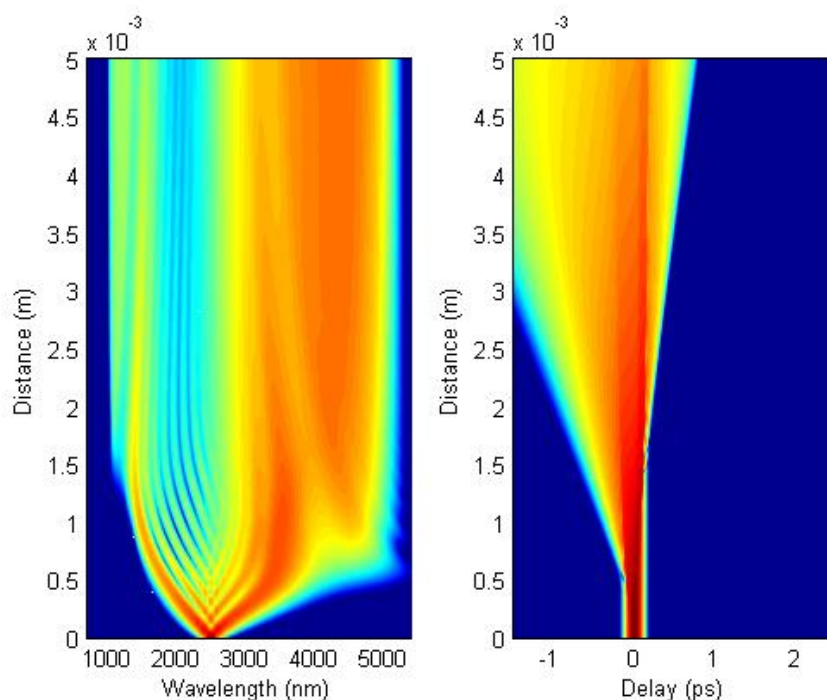## III.3.2 Effect of Self-steepening on SC generation



**Fig III.11 :** Spectral and temporal evolution over 5 mm waveguide length In case Raman exist and shock (Self-Steepening) is absence.

The purpose of simulation replication is to learn how the nonlinear effects contribute to extend the spectrum. We have done the second simulation with initial pulse at Peak Power 10 kw and pulse duration at FHWM = 100 fs propagating over 5 mm waveguide length and Raman exists and Self-steepening is absence. As we've seen from Fig III.11 that absences of shock term has an effect which make the spectral evolution asymmetrically and the spectral broadening increasingly from 0 to 1.5 mm.Without forgetting that OWB responsible too for make the spectral evolution asymmetrically and the spectral broadening.

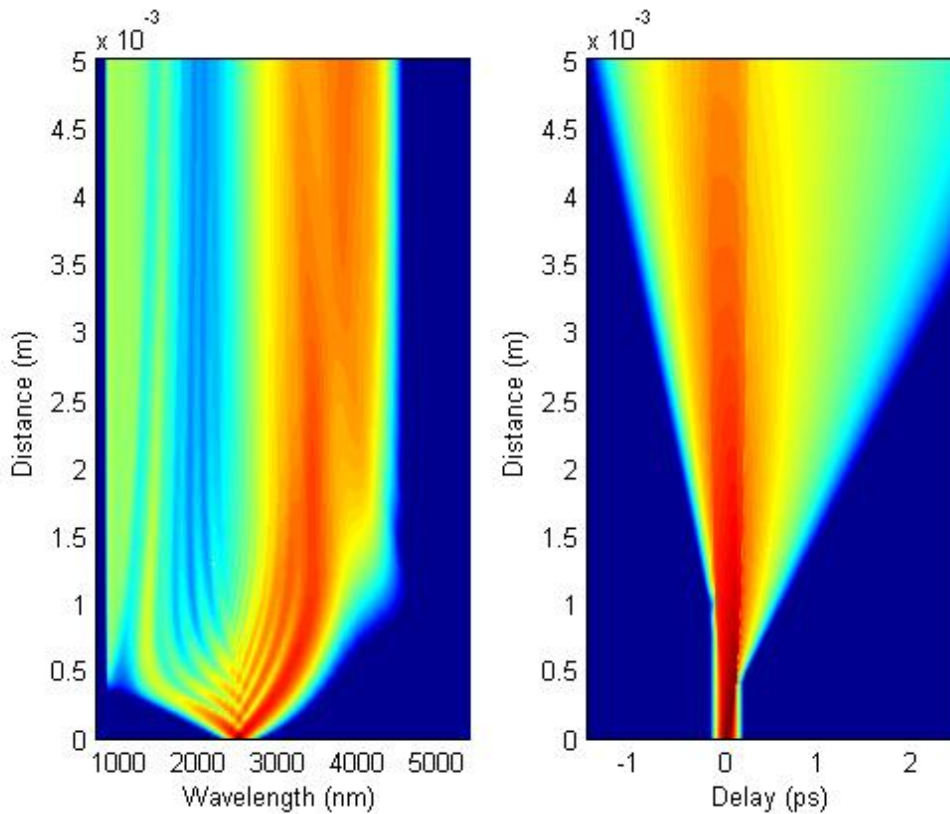## III.3.3 Effect of Raman on SC generation



**Fig III.12:** Spectral and temporal evolution over 5 mm waveguide length In case Raman is absence and shock (Self-Steepening) exist.

We have done the third simulation with initial pulse at Peak Power 10 kw and pulse duration at FHWM = 100 fs propagating over 5 mm waveguide length, and Raman is absence and Self-Steepening exists. As we've seen from Fig III.12 that in case Raman is absence andshock exists there areno changes according to first simulation (Raman and shock are existing).

## III.3.4 Effects of Raman and Self-steepening are absences in SC generation
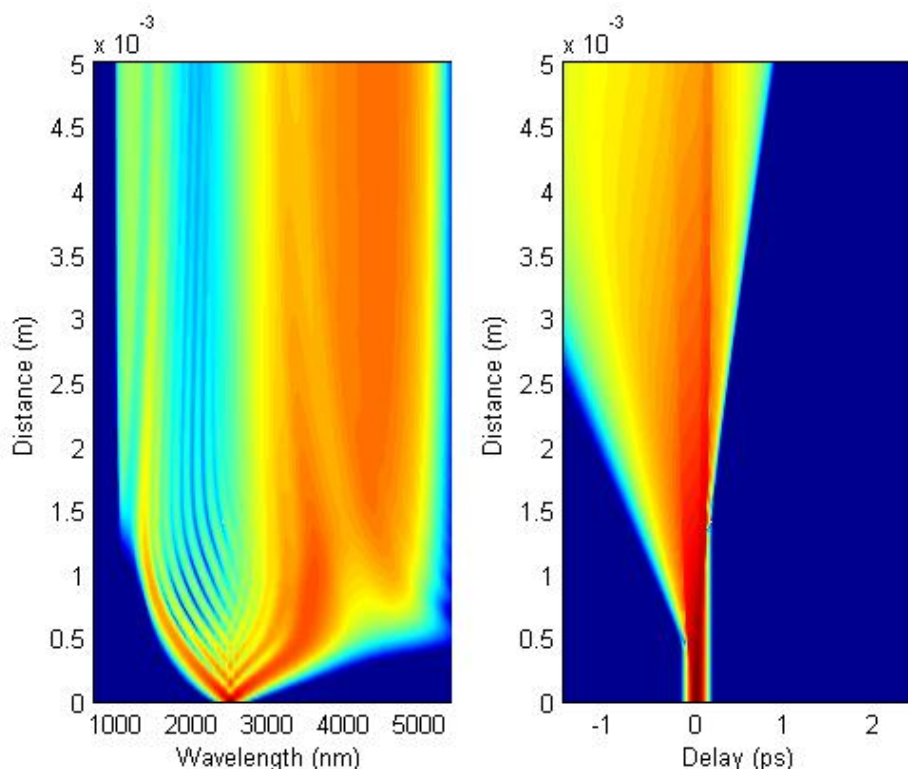


**Fig III.13:** Spectral and temporal evolution over 5 mm waveguide length in case Raman and shock (Self-steepening) are absences.

We have done the forth simulation with initial pulse at Peak Power 10 kw and pulse duration at FHWM = 100 fs propagating over 5 mm waveguide length, and Raman and Self-steepening are absences.As we've seen from Fig III.13 that this simulation give us the same results with second simulation (Raman is absence and shock exists). After neglecting Raman and shock, the GNLSE equation become NLSE (Nonlinear Schrödinger Equation).

As conclusion, we've seen that if Raman exists or not does not have aneffect in spectral evolution but shock (Self-steepening) and Optical Wave Breaking(OWB)have a big effects and Contributes for spectral broaden, so in the normal regime (ANDi), Self-Phase Modulation (SPM) and Optical WaveBreaking (OWB) are responsible for create the spectral broadening.

## III.4 Effects of the Power and FWHM on SC generation

## III.4.1 For Pulse duration FWHM = 50 fs



**Fig III.14 :** Spectral evolution over 5 mm waveguide length of a Gaussian pulse with a peak power of: (a) 10 kW, (b) 15 kW, (c) 20 kW and (d) 25 kW, respectively.
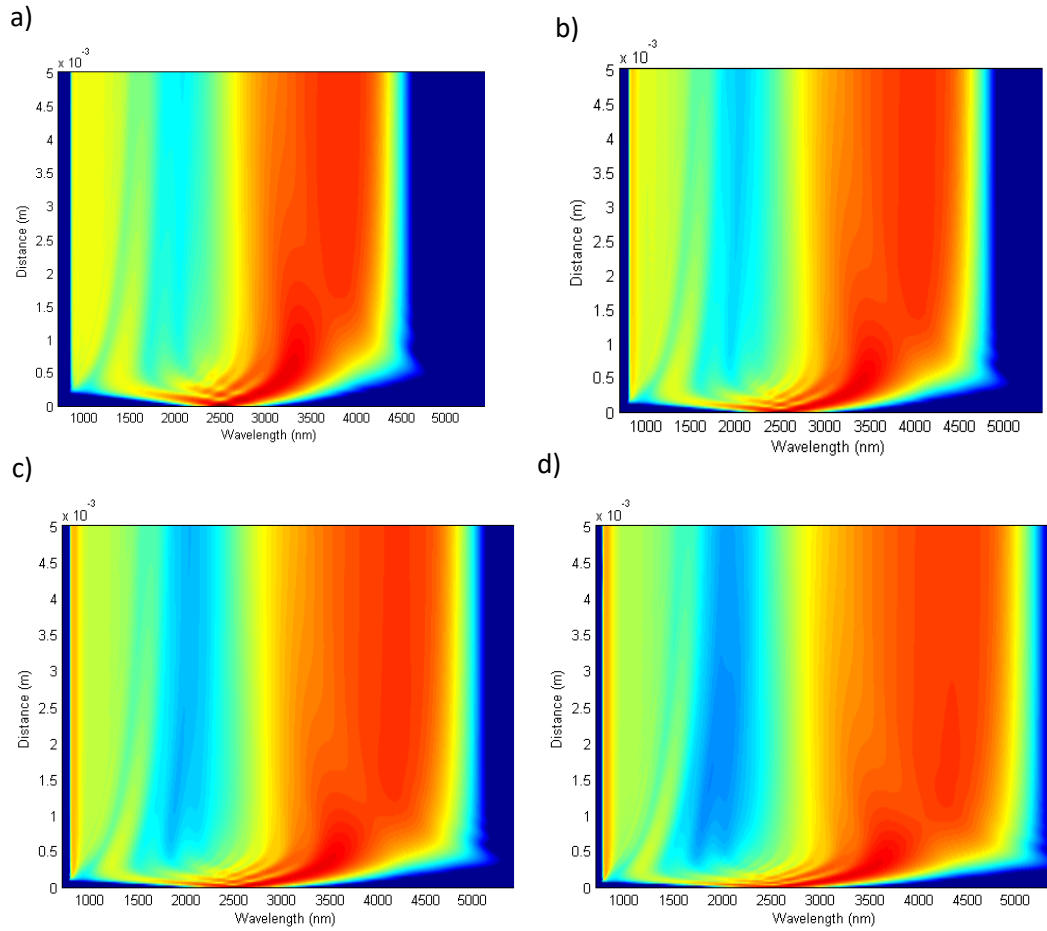
## III.4.2 For Pulse duration FWHM = 100 fs



**Fig III.15 :** Spectral evolution over 5 mm waveguide length of a Gaussian pulse with a peak power of: (a) 10 kW, (b) 15 kW, (c) 20 kW and (d) 25 kW, respectively.

## III.4.2.1 Spectrums at different Powers
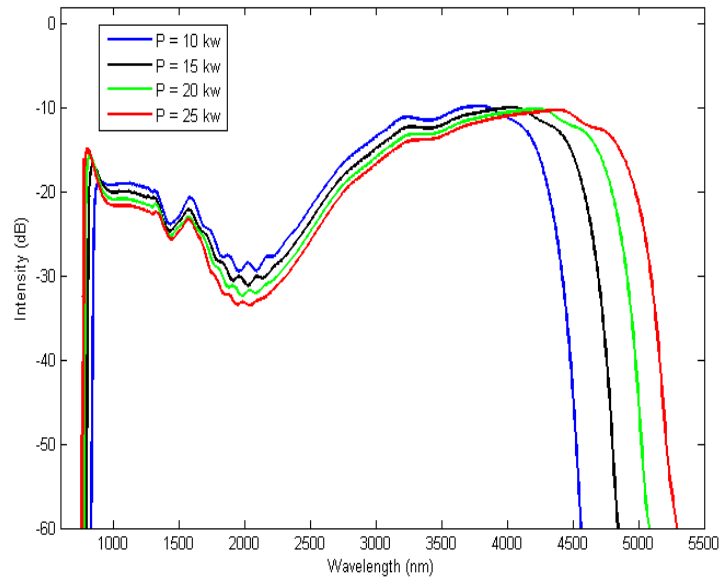


**Fig III.16 :** the different spectrums of the SC generation process at different Powers.

We have done first simulation again But by focusing on the shape of the spectrum at different Powers with initial pulse duration at FHWM = 100 fs, propagating over 5 mm waveguide length, as we can see Fig III.16: shows the different spectrums of the SC generation process at different Powers. As it can be seen that by increasing the initial peak power, the output spectrum width increases too, the pulse form changes a little bit.

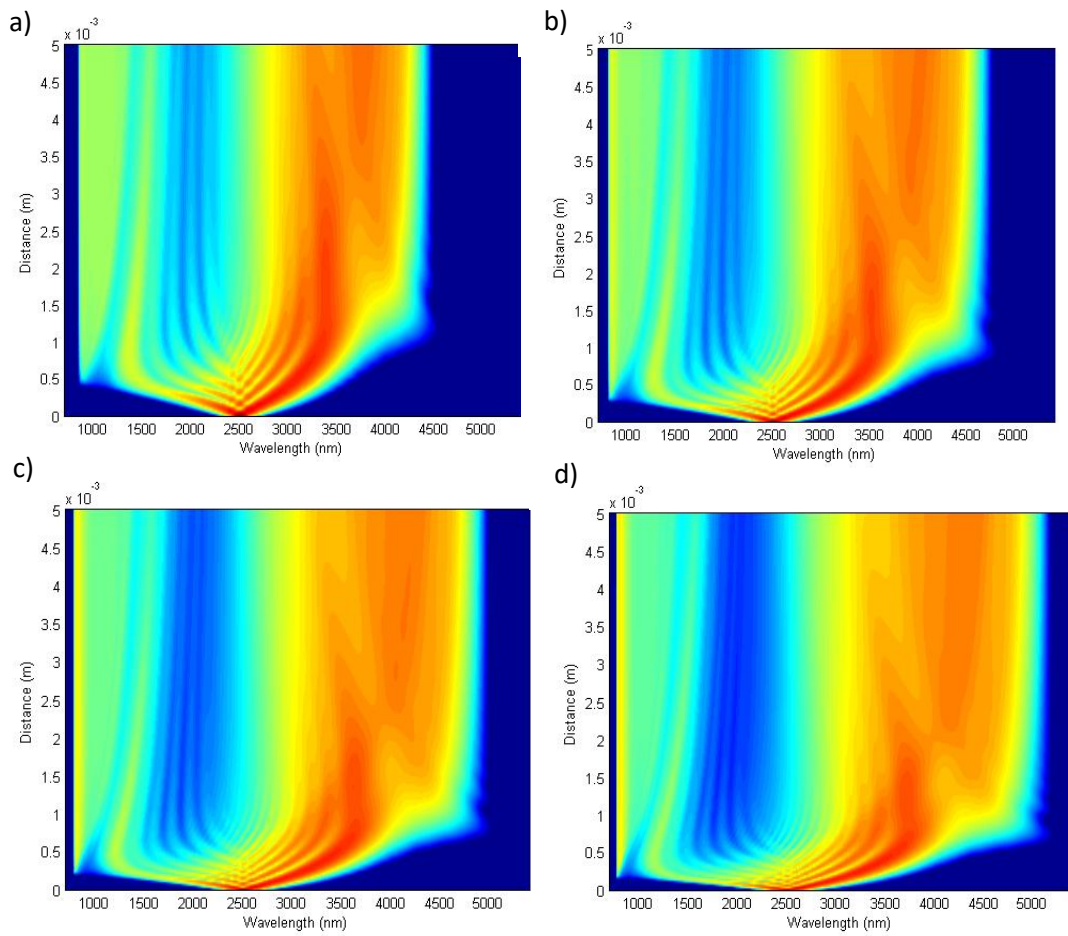## III.4.3 For Pulse duration FWHM = 150 fs



**Fig III.17 :** Spectral evolution over 5 mm waveguide length of a Gaussian pulse with a peak power of: (a) 10 kW, (b) 15 kW, (c) 20 kW and (d) 25 kW, respectively.
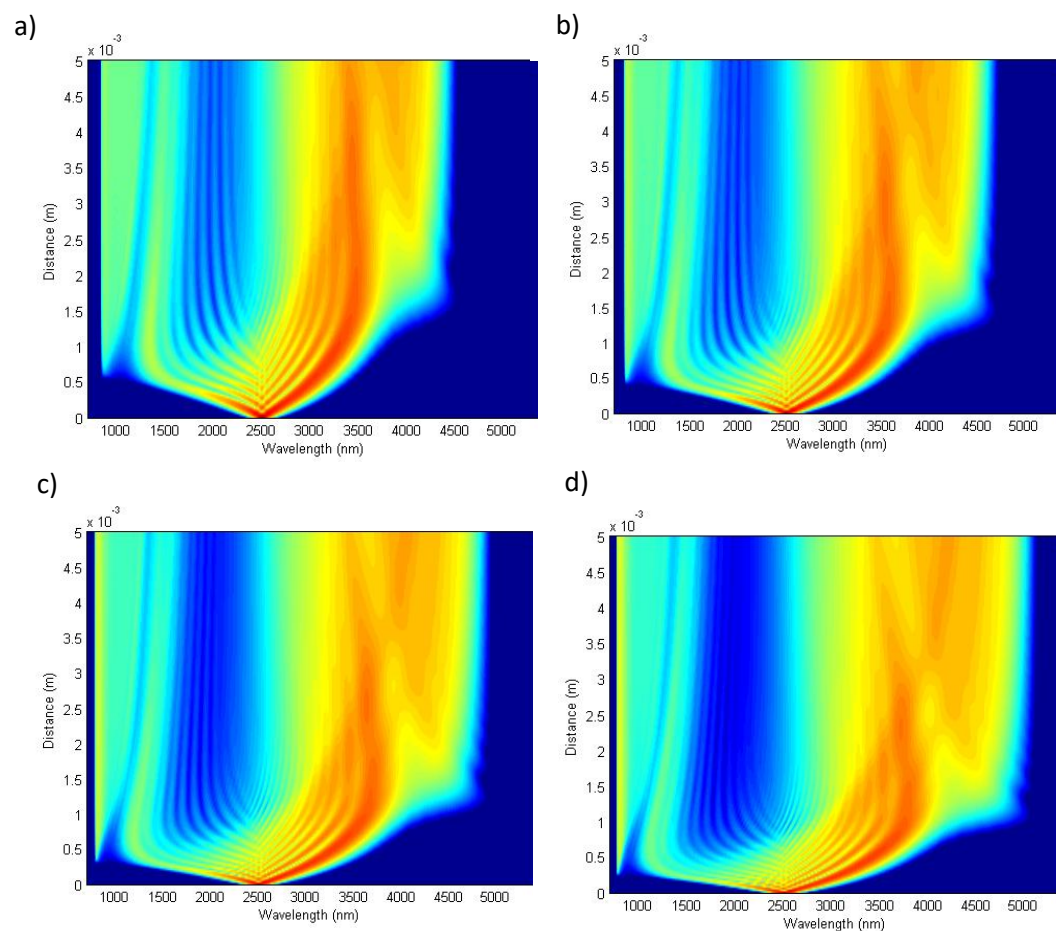
The effect of the initial pulse peak power on the output spectrum width is investigated. Simulations are performed with a pulse with different values of FWHM (50 fs,100 fs,150 fs) and a peak power of 10 kW,15 kW, 20 kW and 25 kW, respectively.

All figures (a)–(d) shows the spectral evolution of the SC generation process over the propagation distance with different values of the peak power. As it can be seen, by increasing the initial peak power, the output spectrum width increases too, where the both sides of the pump wavelength are amplified stronger than the mid-section of the generated spectrum. Moreover, for a peak power of 25 kW, SC spectra

extending to the mid infrared region and spanning 4600 nm in the range from 700 nm to 5300 nm is successfully obtained, along with smooth spectral profile.

According to these Figures (III.11,III.12, III.13, III.14, III.15, III.17) shown at the top, it can be observed that when FWHM is increasing, the OWB appearing point increases too and the largest spectral is first one (50 fs, 25kw ).
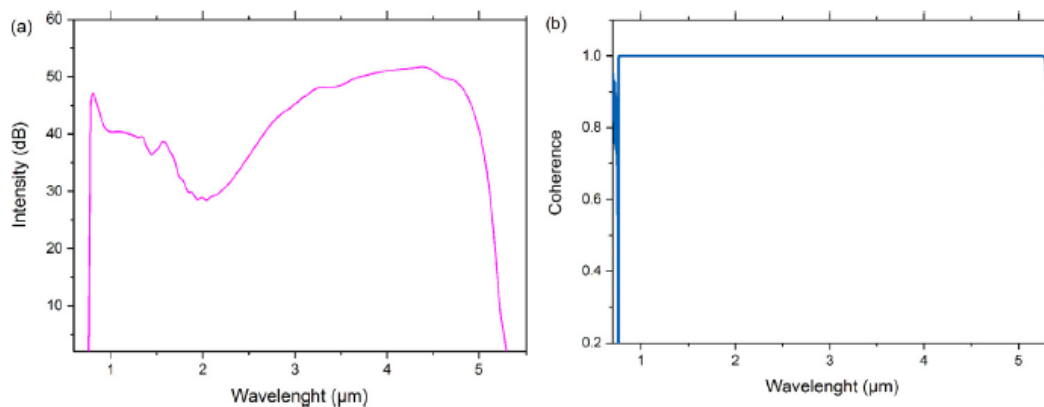
## III.5 Coherence



**Fig III.18:** (a) Generated SC spectrum with an input pulse with a peak power and FWHM of 25 kW and 100 fs, respectively. (b) Corresponding degree of coherence.

Fig III.18 shows the SC generated over 5 mm of the waveguide length employing a pulse with a peak power and FWHM of 10 kW and 100 fs, respectively and the corresponding first-order degree of coherence calculated from 50 independent realizations. As expected, the spectrum is perfectly coherent over the entire spectral range. This high spectral coherence is attained due to the elimination of soliton effects by pumping in the normal dispersion regime. Thereby, spectral broadening is mainly achieved through SPM which is a deterministic process that maintains the input pulses coherence.

# Conclusion

We have numerically demonstrated broadband and coherent SC generation in ANDi ridge waveguide. The proposed dispersion engineered waveguide consists of $As_2S_5$ ChG strip deposited on $MgF_2$ substrate and air acting as an upper cladding. The linear and nonlinear optical properties have been calculated and optimized by using a fully vectorial finite-difference in the frequency-domain (FDFD) method. The numerical results indicate that ANDi profile is obtained over the entire computational domain with a zero dispersion around 2 µm. Besides, the proposed structure exhibits high nonlinearity up to $2.2 \times 10^4$ $w^{-1}km^{-1}$ . Such high nonlinear coefficient is obtained due to the small effective mode area and the high nonlinear refractive index. Furthermore, the SC generation at 2.5 µm is simulated by solving the Non Linear Schrödinger Equation (GNLSE) and using the Split Step Fourier Method (SSFM).

Simulations have shown that spectral broadening is realized due to SPM and OWB. and we saw effects of Power and pulse duration FWHM and we've seen the impact of the presence and absence of nonlinear effects in SC generation. A broad and perfectly coherent ultra-flat SC spectrum extending from 700 to 5300 nm is successfully generated by using a 25 kW peak power and 50 fs input pulse in only 5 mm waveguide length.Owing to its interesting properties, the proposed $As_2S_5$ ChG based waveguide is found to be suitable as an on-chip SC source for various applications such as gas sensing, frequency comb generation and ultrafast optical switching.

# References

[1] Tonglei Cheng, Ryo Usaki, Zhongchao Duan, Weiqing Gao, Dinghuan Deng, Meisong Liao, Yasuhire Kanou, Morio Matsumoto, Takashi Misumi,Takenobu Suzuki, Yasutake Ohishi, "Soliton self-frequency shift and third-harmonic generation in a four-hole As2S5microstructured optical fiber,Opt", Express 22, 3740–3746, (2014), http://dx.doi.org/10.1364/OE.22.003740.

[2] M.R. Karim, B.M.A. Rahman, Govind P. Agrawal, "Mid-infrared supercontinuum generation using dispersion-engineered Ge11.5As24Se64.5chalcogenide channel waveguide", Opt. Express 23, 6903–6914, (2015), http://dx.doi.org/10.1364/OE.23.006903.

[3] Abdelkader Medjouri.et al."Design and optimization of $As_2S_5$ chalcogenide channel waveguide for coherent mid-infrared supercontinuum Generation" .Elsevier, 25 Oct.p. 4, (2017).

[4] Alexander M. Heidt, "Pulse preserving flat-top supercontinuum generation in all-normal dispersion photonic crystal fibers", J. Opt. Soc. Am. B 27(2010) 550–559, http://dx.doi.org/10.1364/JOSAB.27.000550.

[5] W. J. Tomlinson, R. H. Stolen, and A. M. Johnson, "Optical wave breaking of pulses in nonlinear optical fibers," Opt. Lett. 10, 457-459, (1985).

https://www.osapublishing.org/ol/abstract.cfm?URI=ol-10-9-457.

[6] S. O. Iakushev1, IEEE, et al. "Optical Wave Breaking Cancelation and Formation of Quasi-Parabolic Ultrashort Pulses", In: proceedings of the 2010 LFNM International Conference on Laser & Fiber-Optical Networks Modeling, 12-14 September, 2010, Sevastopol, Ukraine.

[7] Christophe Finot, Bertrand Kibler, Lionel Provost, Stefan Wabnitz, Beneficial "impact of wave-breaking for coherent continuum formation in normallydispersive nonlinear fibers", J. Opt. Soc. Am. B 25, 1938–1948, (2008),http://dx.doi.org/10.1364/JOSAB.25.001938.

[8] Alexander M. Heidt, "Pulse preserving flat-top supercontinuum generation in all-normal dispersion photonic crystal fibers", J. Opt. Soc. Am. B 27, 550–559, (2010),http://dx.doi.org/10.1364/JOSAB.27.000550.

[9] D. Anderson, M. Desaix, M. Lisak, M.L. Quiroga-Teixeiro, "Wave breaking in nonlinear-optical fibers", J. Opt. Soc. Am. B 9, 1358–1361, (1992),http://dx.doi.org/10.1364/JOSAB.9.001358.

# GENERAL CONCLUSION

The objective of this research was to study Broadband laser source on an optical chip using a chalcogenide glass waveguide employing highly nonlinear chalcogenide (ChG) between near-infrared and mid-infrared regime. This was done in ChG planar waveguides (ridge waveguides) and it is considered for designing such SC sources which could be used for near infrared to mid-infrared applications.

The waveguides proposed for designing SC sources were optimized by applying rigorous numerical procedure such as the finite-difference frequency-domain (FDFD) approach and the results obtained by this approach have been utilized for numerically solving the generalized nonlinear Schrödinger equation (GNLSE) to study broadband SC generation.

First step, we were interested in the study of the main elements related to the generation of SC on chip, that is needed to understand the work presented in this thesis. For an understanding in general the photonic integrated Circuits (PICs) as well as types of optical waveguides and overview for supercontinuum generation SCG and its types, and chalcogenide material and its features.

Second step, we were interested in the study of the main effects that take place during the propagation of light waves in the ridge waveguide. For an understanding of the linear (losses and dispersion) and nonlinear phenomena (the kerr effect, Self-Steepening and Raman scattering) as well as their effects during propagation of optical signal inside the waveguide it is necessary to introduce the GNLSE that governs the propagation of optical field in the waveguide. Finally, a few of the most relevant nonlinear effects and concepts responsible for propagation dynamics of SC generation have been reviewed.

in the last step, we have numerically demonstrated Broadband laser source on an optical chip using a chalcogenide glass in ANDi ridge waveguide (in normal regime D < 0), The waveguide structure is optimized to exhibit an all normal dispersion (ANDi) profile over the entire computational domain by properly adjusting its high and width. and we've seen that the proposed dispersion engineered waveguide consists of $As_2S_5$ ChG strip deposited on $MgF_2$ substrate and air acting as an upper cladding.

The linear and nonlinear optical properties have been calculated and optimized by using a fully vectorial finite-difference in the frequency-domain (FDFD) method. The numerical results indicate that ANDi profile is obtained over the entire computational domain with a zero dispersion around 2 μm. Besides, and we see that the proposed structure exhibits high nonlinearity up to $2.2 \times 10^4$ $w^{-1}km^{-1}$. Such high nonlinear coefficient is obtained due to the small effective mode area and the high nonlinear refractive index. Furthermore, we've done the SC generation at 2.5 µm is simulated by solving the generalized Non Linear Schrödinger Equation (GNLSE) and using the Split Step Fourier Method (SSFM).

Simulations have shown that spectral broadening is realized due to SPM and OWB in normal regime. and we saw effects of Power and pulse duration FWHM and we've seen the impact of the presence and absence of nonlinear effects in SC generation.

As we've seen in Simulation results, that a broad and perfectly coherent ultra-flat SC spectrum extending from 700 to 5300 nm is successfully generated by using a 25 kW peak power and 50 fs input pulse in only 5 mm waveguide length. Owing to its interesting properties, the proposed $As_2S_5$ ChG based waveguide is found to be suitable as an on-chip SC source for various applications.